Experimental Measurement Methods for the Evaluation of Degradation in Piezoelectric Ceramics

Dr Markys G Cain, Dr Mark Stewart and Dr Mark G Gee

May 1998

Experimental Measurement Methods for the Evaluation of Degradation in Piezoelectric Ceramics

M G Cain, M Stewart, M G Gee
Centre for Materials Measurement and Technology
National Physical Laboratory
Queens Road, Teddington
Middlesex, TW11 0LW UK

Summary

As part of the DTI programme on the development of test methods for characterisation of advanced materials, project CAM 7 *Electroactive materials properties under conditions of high stress or stress rate,* has the overall aim of defining and improving the measuring framework for electroactive materials which will enable them to be used with greater confidence by UK industry. Earlier reports within CAM7 have described measurement methods for piezoelectrics at high electrical stresses. This report discusses the extension of those methods to allow measurements to be carried out with superimposed mechanical stresses, and also the extended use of these methods with repeated exposure to measure the degradation of performance.

ISSN 1361-4061

National Physical Laboratory Management Ltd
Teddington, Middlesex, TW11 0LW, UK

Approved on behalf of the Managing Director, NPL, by
Dr C Lea, Head of Centre, Centre for Materials Measurement and Technology

Table of Contents

INTRODUCTION 3

DEGRADATION PHENOMENA 3
FATIGUE IN PIEZOELECTRIC CERAMICS 4

EXPERIMENTAL CONDITIONS AND FATIGUE RESULTS 5

EXPERIMENTAL FATIGUE SYSTEMS 5
EXPERIMENTAL CONDITIONS 5
CYCLIC MECHANICAL STRESS - HIGH MECHANICAL STRESS/FEW CYCLES 6
STATIC MECHANICAL STRESS - LOW LEVEL PERMITTIVITY 7
ELECTRICAL STRESS - EFFECT OF STATIC STRESS ON HIGH DRIVE LEVEL PROPERTIES 11
POLARISATION LOOP MEASUREMENT 11
IMPEDANCE SPECTROSCOPY 16
Resonance determination of experimental system 16
Static Mechanical Loading - Dielectric Property Measurements 18
ELECTRICAL FATIGUE - DIELECTRIC PROPERTY MEASUREMENTS 21
MECHANICAL FATIGUE: HIGH STRESS RATE MEASUREMENTS 22
MECHANICAL FATIGUE - MEASUREMENT OF D_{33} 23

CONCLUSIONS 28

REFERENCES 29

APPENDIX 1: EXPERIMENTAL PLAN AND QUESTIONNAIRE RETURNS. 30

Table of Figures

Figure 1: Schematic stress-strain and stress-polarisation curves. (Shaufele et al. 1996) 4
Figure 2: Change in effective k_p with mechanical cycling of a soft material for various stress amplitudes. 6
Figure 3: Change in normalised capacitance at 1kHz for mechanical cycling with a stress amplitude of 64 MPa, for a soft 5H and hard 4D material. 7
Figure 4: Low field permittivity at 1kHz under an applied axial load with several repeated runs for hard PC4D material (sample dimensions 5mm long, 10mm diameter). 8
Figure 5: Effect of different thickness samples on low field permittivity at 1kHz under mechanical loading (sample diameter 10mm). 9
Figure 6: Effect of adding 10mm long, 10mm diameter aluminium spacers on the low field permittivity of a PC4D material under mechanical loading (sample diameter 10mm). 10
Figure 7: Low field permittivity at 1kHz under an applied axial load for a soft 5H material (sample 5mm long, 10mm diameter). 10
Figure 8: Schematic of sample holding fixture 11
Figure 9: Simultaneous a)P-E and b)S-E loops for a soft PC5H material, at 1 Hz for axial stresses of 0, 6, 12 and 32MPa. Frequency 1Hz, sample dimensions 5mm long, 10mm diameter. 12
Figure 10: Applied voltage and strain output for the first applied field cycle after releasing the load from 32MPa to zero. Frequency 1Hz, sample dimensions 5mm long, 10mm diameter 13
Figure 11: d_{33} against applied axial stress for a 10mm thick 10mm diameter hard PC4D sample, for loading and for unloading. 14
Figure 12: Stress strain curve for sample in Figure 11 15
Figure 13: High voltage dielectric interface measuring equipment for electrical fatigue measurements 16
Figure 14: Resonance scan for hard material in E-Rig fatiguing system 17
Figure 15: Resonance scan for soft material in E-Rig fatiguing system 17
Figure 16: Permittivity as a function of static load and electrical field for PC4D hard material at a frequency of 100Hz 18
Figure 17: Loss tangent for PC4D hard material showing increase with electric field and increase with static loading. 19
Figure 18: Loss tangent for PC5H soft material showing increase with electric field and decrease with static loading. 20
Figure 19: permittivity as a function of static load and electrical field for PC5H soft material 20
Figure 20 (a): Electrical Fatigue for PC5H (b): Electrical Fatigue for PC4D 21
Figure 21: Engineering drawing of stiff loading rig. 22
Figure 22: Photograph of Plint rig and magnetostrictive actuator set up for fatigue measurements 22
Figure 23: Photograph of E-rig. 23
Figure 24: Schematic set up for the measurement of d33. 24
Figure 25: Piezoelectric coefficient measured using the E-rig system previously described. 25
Figure 26: Piezoelectric coefficient, d_{33} with amplitude (pk/pk) of ac pressure. 26
Figure 27: Mechanical Fatigue for soft PC5H measured via d_{33}. 26
Figure 28: Mechanical fatigue using Plint system and magnetostrictive actuator 27

Experimental Measurement Methods for the Evaluation of Degradation in Piezoelectric Ceramics

Introduction

The electrical and mechanical fatigue exhibited by many piezoelectric and ferroelectric materials continues to limit their applications as actuators and many types of sensors and other functional devices. Fatigue may be described by a decay in the polarisation and coercive field, associated with increasing electrical and/or mechanical stressing cycles. The attempts to explain the mechanisms for fatigue in these materials have been based on intrinsic or extrinsic phenomena including 90° and 180° domain wall motion and/or domain switching, domain pinning via space charge effects, surface deterioration via electric discharge within pores and, ultimately, the generation of microcracks in response to the very large strain accumulation within pores and imperfections.

To demonstrate the effects of electrical and mechanical cyclic stressing on the functional properties of commercial PZT materials, previously described measurement methods (CMMT (A)98 and (A)99) were extended to enable fatigue measurements to be conducted. Mechanical testing systems were specifically designed to perform these tests. The test systems, measurement methods, and some preliminary results are described within this report.

Degradation Phenomena

The terminology used to describe the loss in performance with time (and or stress) of these functional materials is somewhat confusing. It is expedient to simply group all of the various mechanisms together and label them degradation. Although these different mechanisms will be discussed here, it is likely that in real applications where more than one of these mechanisms may be in operation, the distinctions between different mechanisms may become academic.

The most fully understood form of degradation is ageing, where there is a spontaneous loss in the functional performance of the piezo-ceramic with time. This is thought to be due to the progressive rearrangement of domains into more stable configurations. It has an associated activation energy which describes how the ageing accelerates at higher temperatures. The loss in performance is usually logarithmic, and manufacturers will quote ageing characteristics in terms of percentage loss per decade. Often piezoelectric measurements are performed 24 hours after poling, when the initial rapid rate of change in properties is reduced. (Morgan Matroc Ltd).

Under a constant DC electric stress the materials can undergo an increase in conductivity with time (termed resistance degradation). This leads eventually to dielectric breakdown, sometimes called time dependent dielectric breakdown. This phenomena is of most concern for capacitor applications and is one of the limiting factors for reliability of multilayer ceramic capacitors (Waser at al. 1990). This is generally thought to be due to an oxygen vacancy migration towards the cathode creating, in effect, a forward biased p-n junction. Experiments have confirmed that variables that increase oxygen vacancy concentration and mobility, such as acceptor doping, also increase the resistance degradation (Warren et al. 1996).

Fatigue in Piezoelectric ceramics

The term fatigue, in the context of piezoelectric degradation, has been used to describe the loss in performance brought about by either mechanical or electrical loading. However, it is likely that the two mechanisms are very different phenomena. Ferroelectric fatigue caused by the *application* of AC electrical loads leads to the loss of switchable polarisation. This is a result of the progressive inhibition of the motion of domain walls. The mechanisms responsible for this type of degradation have been linked to various phenomena including the entrapment or accumulation and resorption of space charge at the domain boundaries (Chen et al. 1997, Kudzin et al. 1975, Jiang et al. 1993), the growth of oxygen-deficient filaments (Duiker at al. 1990), and domain wall pinning via the motion of electronic charge and ionic defects vis. oxygen vacancies (Chen et al. 1997, Warren et al. 1994). Many of the studies of ferroelectric fatigue are related to thin film memory applications, where the square hysteresis loop is used to good effect as a data storage device (Aoki et al. 1997). Here the loss of switchable polarisation leads to the indistinguishablity of the ‘on’ and the ‘off’ states.

Fatigue has also been used to describe the mechanical failure of piezoelectric materials, at loads below the failure strength, following the application of cyclic mechanical loads, and also indirectly via cyclic electrical loads. Many of the damage mechanisms are similar to those found in mechanically cycling conventional ceramics, but there is the added complication that electrical fields can affect crack growth. The degradation is generally attributed to an accumulation of microcracks forming within the ceramic, and although domain reorientation occurs, this is not, however, linked to microcrack evolution (Hill et al. 1996).

It is not the purpose of this report to attempt to describe such phenomena in detail but rather to describe experimental methods which might offer potential for the measurement of degradation and fatigue.

Most of the degradation phenomena discussed so far have been those that take decades of cycles or a long time to show significant change in properties. Piezoelectric ceramics are commonly poled polycrystalline devices, which can be readily depoled by applying a large electrical or mechanical stress, or by taking the material through its Curie temperature. Several workers have studied the effects of large mechanical stresses on typical piezo-ceramic materials (Shaufele et al. 1996 and Cao et al. 1993). Figure 1 shows the expected strain and depolarisation behaviour for a PZT type material measured under uniaxial stress. In the initial linear region (A-B) the material behaves linearly, with the polar direction parallel to the applied stress. In the region C-D the domains start to switch, giving rise to a non-linearity and it is only linear again in

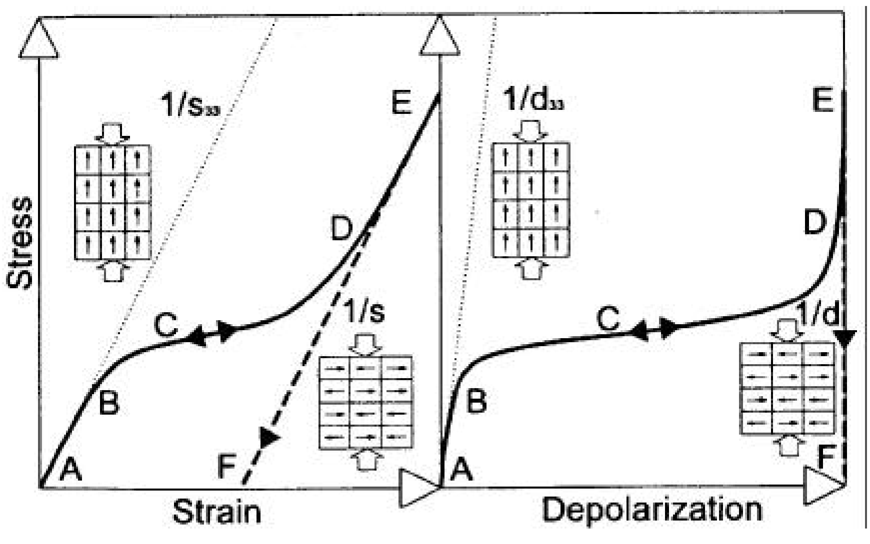

Figure 1: Schematic stress-strain and stress-polarisation curves. (Shaufele et al. 1996)

the region D-E, where the polar direction is now perpendicular to the applied stress. When the stress is removed (A-F) the material has been left with a remnant strain and polarisation. In practice, the first linear region extends up to around 20MPa for soft and 80MPa for hard materials, with full depolarisation requiring up to 400MPa stress levels. Clearly, 400MPa is a large stress to apply to a piezo-ceramic. However, once the initial linear region is exceeded, there is always some remnant strain and polarisation. This may be accumulated by driving materials around this load cycle several times. To investigate this, a series of experiments were conducted in which materials were cycled through a relatively high load.

Experimental Conditions and Fatigue Results

Experimental Fatigue Systems

The loading configurations that have been developed at NPL are based on two similar rig systems. Both systems can apply compressive static forces to piezoelectric test pieces of various geometries and sizes. The driving field may be electrical or mechanical or both. Several actuators based on piezoelectric stack actuators (Physik Instrumente) and magnetostrictive actuators (Magnetostrictive Inc.) may be incorporated within the frame of the rigs. The rigs have been designed to accommodate the actuation device, associated load measuring sensors (such as resistive bridge load cells or high stiffness quartz load cells), displacement measuring sensors (optical, capacitative and strain gauge technologies), and charge detection systems (virtual earth or open circuit configurations). The various measurement methods which have been demonstrated with the fatigue rigs will be described in this report. This is a deliverable to the customer (DTI) labelled Milestone 4 - Experimental Measurement Methods for the Evaluation of Fatigue in Piezoelectric Ceramics.

Experimental Conditions

The various experimental conditions developed and parameters which have been measured are described in Table 1. Mechanical and electrical loads of a static and dynamic nature have been applied to the piezoelectric ceramic materials. The response and degradation of the materials to the imposed stress has been assessed through the measurement of dielectric properties, strain, polarisation and charge. The following sections are based on the methodology summarised in Table 1.

Input		***Measurement parameters***
Mechanical Loads	Static - imposed strain Dynamic (low electrical field)	Relative permittivity (capacitance) Loss tangent Polarisation with field P(E) Strain Charge
Electrical Loads	Dynamic / dispersive Static imposed mechanical loads	
Time / fatigue	Number of cycles History	

Table 1: Experimental conditions and measurement scenario

Cyclic mechanical stress - high mechanical stress/few cycles

Mechanical cycling was carried out on a selection of piezo-ceramic materials in the form of discs 10mm diameter and thickness of 1, 2 and 5mm. Loads of up to 5, 10, 15 and 20kN were applied in a sinusoidal manner at a frequency of 0.1Hz using an Instron mechanical testing machine with a conventional screw driven actuator. Tests were interrupted after each cycle and a selection of electrical tests were carried out using an HP4192A impedance analyser.

Figure 2 shows measurements of k_p determined from the radial resonance peak for a soft PZT 5A material for stresses corresponding to 127, 190 and 255MPa. This material is one of the 'harder' soft compositions; and although 255MPa results in large scale depoling occurring after the first cycle, the drop off in k_p is more gradual at 127 and 190MPa.

There are a number of transient events that occur during the mechanical cycling causing a rapid drop off in the k_p. This is due to the fracture and loss of small pieces around the edge of the sample. Nevertheless, the behaviour for the repeated curves is reasonably consistent, with the fractures causing an offset in the curve. In contrast to the drop in k_p, the permittivity of the samples increases with increasing cycles, at least initially for the PC5H material. Figure 3 shows the normalised capacitance for a soft 5H and a hard 4D material with an applied cyclic load of 5kN (64MPa). The soft material shows a rapid increase of almost 10% over the first few cycles, followed by a gradual decrease, whereas for the hard material the capacitance is still increasing after 50 cycles.

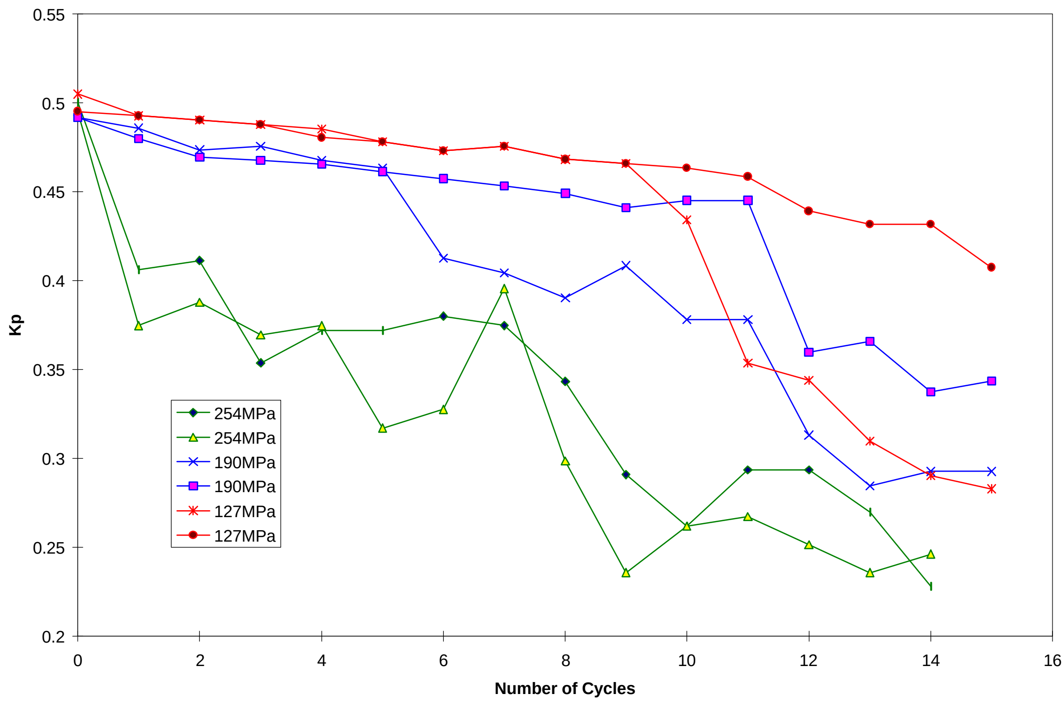

Figure 2: Change in effective k_p with mechanical cycling of a soft material for various stress amplitudes.

From the preceding experiments it is clear that at stresses of above 60MPa gross mechanical depolarisation occurs producing rapid degradation in functional performance, and even at 60MPa repeated cyclic application at these stresses increases the degradation. The hard and soft materials behave differently with the consequence that experiments on the soft materials need to be confined to lower stress levels.

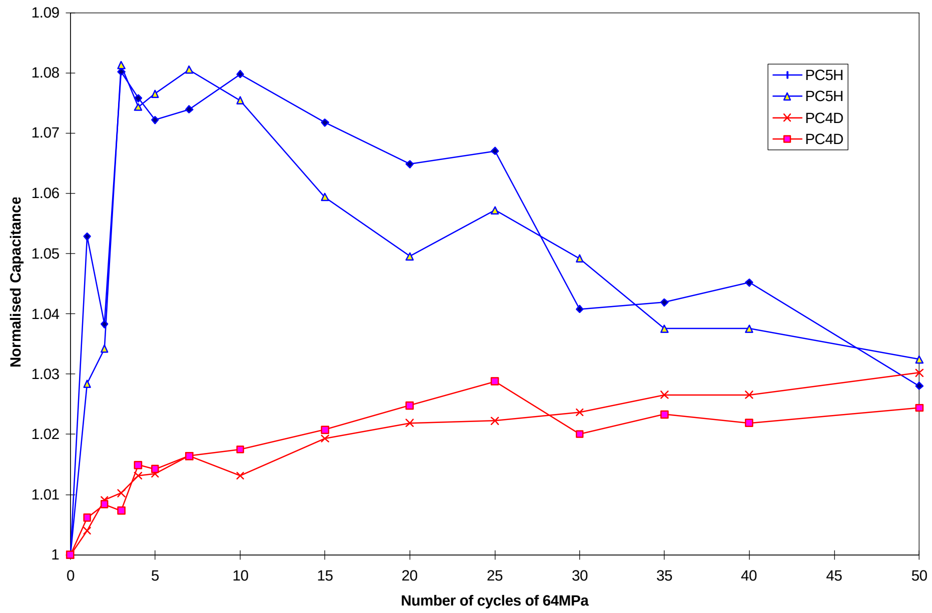

Figure 3: Change in normalised capacitance at 1kHz for mechanical cycling with a stress amplitude of 64 MPa, for a soft 5H and hard 4D material.

Static mechanical stress - low level permittivity

In many real actuator applications the piezo-ceramic will be under some form of static mechanical pre-stress which will then be driven with a high electrical field, i.e. much greater than 1V/mm. In order to examine some of the experimental effects of applying a static stress a simpler experiment is to measure the low level properties, namely the permittivity and loss.

Static stresses have been applied with a conventional mechanical testing machine, with the load measured by a strain gauge load cell. The permittivity and loss were measured using a HP4192A and a Solartron 1260 at 1kHz and at an applied voltage of 1V rms. In order to capture a waveform of permittivity against electrical stress, the stress was set to cycle from zero to the maximum load at a frequency of 0.001Hz, and the capacitance, loss and applied load were recorded every second with a computer logger. Ideally the applied load should have been stepped, the sample allowed to stabilise for a period of time, and then the capacitance and loss recorded. However it was difficult to control the applied load with the logging program, and experimentation with the frequency of the applied load showed that at 0.001Hz with the load range chosen this stabilisation was not necessary.

Figure 4 shows a series of stress cycles with increasing maximum stress and repeated application on a 4D cylinder 5mm long 10mm diameter. The stress cycles with a maximum of 64MPa show reasonably linear increase in permittivity with increasing stress, although there is significant hysteresis on removing the load. There is also a 'ratcheting' increase in the zero stress permittivity with repeated cycling, with the largest jump coming after the first cycle. If samples are left to recover for 24 hours or so there is a recovery of the pre-stressing permittivity value after excursions to 64MPa. Cycles to higher stresses of 128 and 256MPa

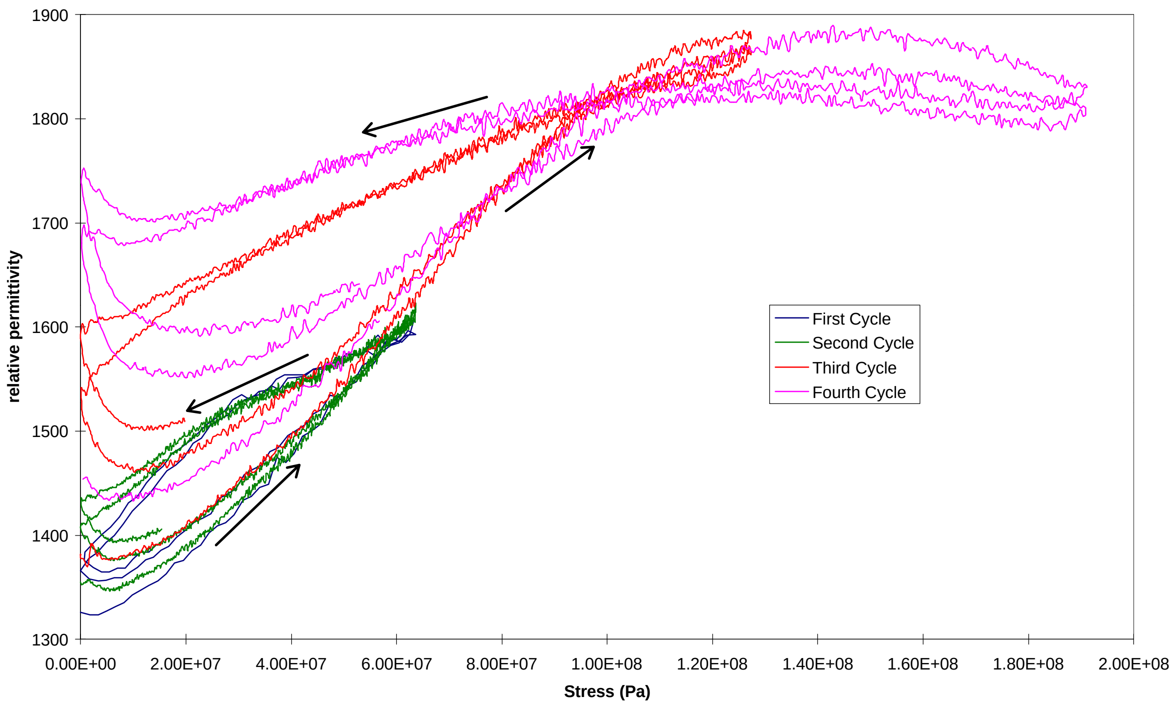

Figure 4: Low field permittivity at 1kHz under an applied axial load with several repeated runs for hard PC4D material (sample dimensions 5mm long, 10mm diameter).

show more non linear behaviour, far greater zero stress permittivity, and the subsequent curves do not follow each other, indicating that degradation has occurred. If this is compared with the expected stress polarisation behaviour it would appear that at above 64MPa there is significant depolarisation.

There are two perceived difficulties with the experiment as described above. Firstly, the use of flat disc shape samples, rather than long cylinder shaped samples can lead to inhomogeneities in the stress field. Secondly the measurement of the permittivity is via the application of a sinusoidal electrical field, which introduces a stress wave in the sample which, depending on the resonance behaviour of the complete measurement set-up, can affect the magnitude of the permittivity. However, as the magnitude of the permittivity close to zero stress was similar to the zero stress permittivity, this was not thought to be a problem. Also, although most tests were carried out at 1 volt, tests at 100mV gave similar (albeit noisier) results indicating that the displacement generated by the measurement was not affecting results. This is more likely to be a problem when measuring the high field properties. One possible solution here is to have two identical samples back to back in the experimental arrangement, so that the displacements generated cancel out and the measurement field does not produce a stress wave (Krueger, 1967).

In order to investigate the homogeneity of the stress field a series of tests using samples with different thickness was carried out. Figure 5 shows the permittivity against load curves for 1, 2 and 5mm thick samples. There is, indeed, a noticeable effect of different sample thickness, with a flattening out of the permittivity increase with applied load as the thickness is reduced. The difference in zero load values is not significant because they are different samples with different poling conditions and histories. For the measurements, it would be convenient to stipulate that all samples should have a thickness to width ratio of at least 1:1. However, as most actuators

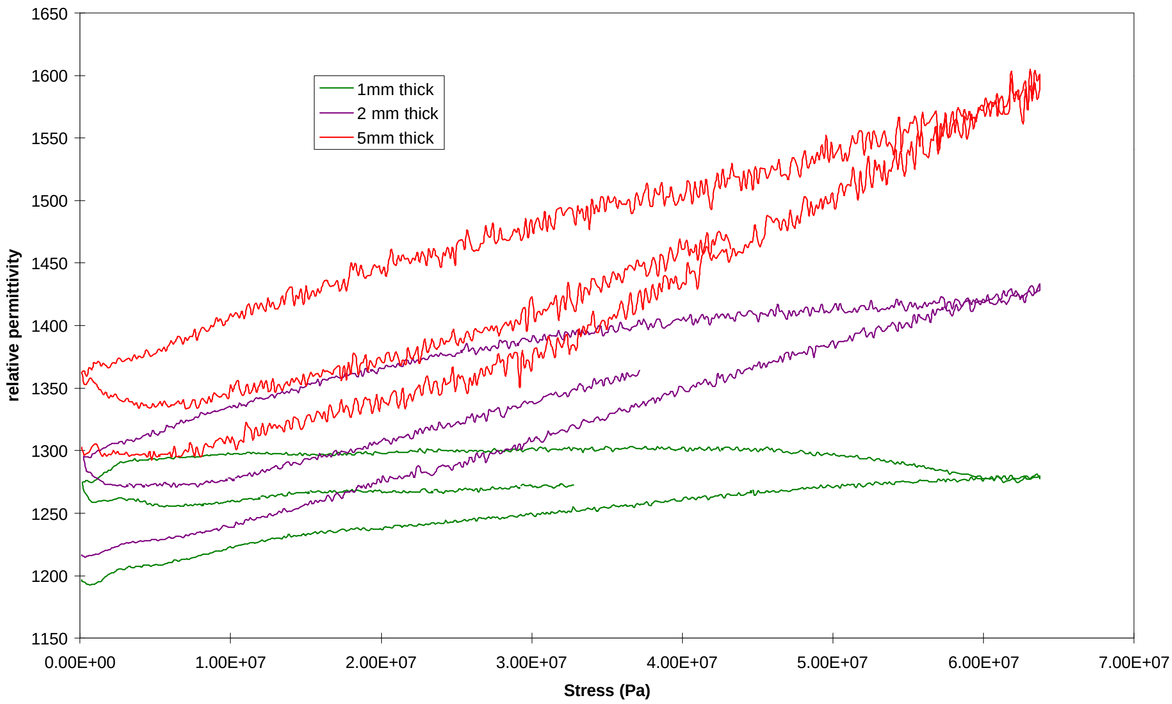

Figure 5: Effect of different thickness samples on low field permittivity at 1kHz under mechanical loading (sample diameter 10mm).

tend to be based on designs using disc shapes for the piezoelectric elements, rather than cylinders, and since disc forms are lower cost and achieving higher fields is simpler, it would be useful if experiments could continue with these shapes. A parallel study under DTI-funded CAM7 is being carried out to examine the stress state within these materials as they undergo testing using finite element modelling.

It may be possible to obtain a more uniform stress state in the material by extending the effective length of the sample by the inclusion of similar stiffness material at either end (Paul Michelis, Personal Communication). Thus, sandwiching samples between two 10mm long 10mm diameter aluminium cylinders tended to decrease the effect of having thinner samples (Figure 6). This is particularly true as the load increases.

For the soft material, the behaviour is reversed with the low field permittivity decreasing with increasing uniaxial stress (Figure 7). The total percentage change is much less, so that although the maximum increase in permittivity for the hard material is of the order 25%, the maximum decrease for the soft material is around 5%, although the stress levels for the soft material were kept to 12MPa. This might seem to contradict the high stress low cycle capacitance measurements (Figure 3); however, those were conducted at low field, resulting from remnant changes in the material, whereas the present measurements are performed under a high static stress.

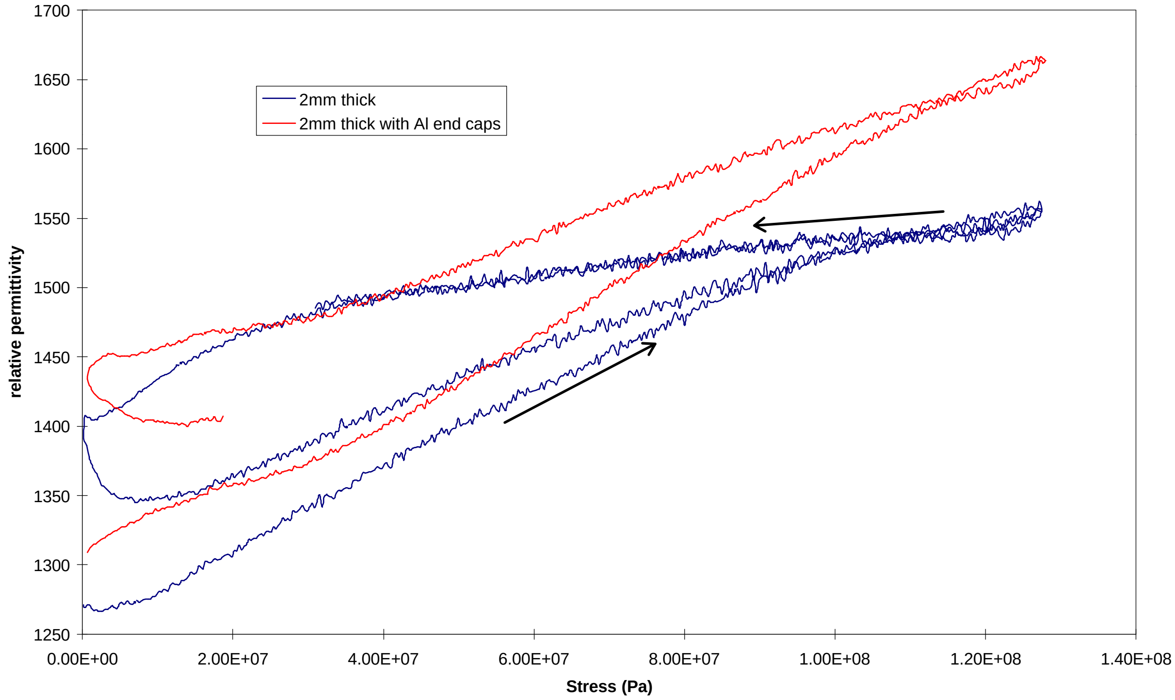

Figure 6: Effect of adding 10mm long, 10mm diameter aluminium spacers on the low field permittivity of a PC4D material under mechanical loading (sample diameter 10mm).

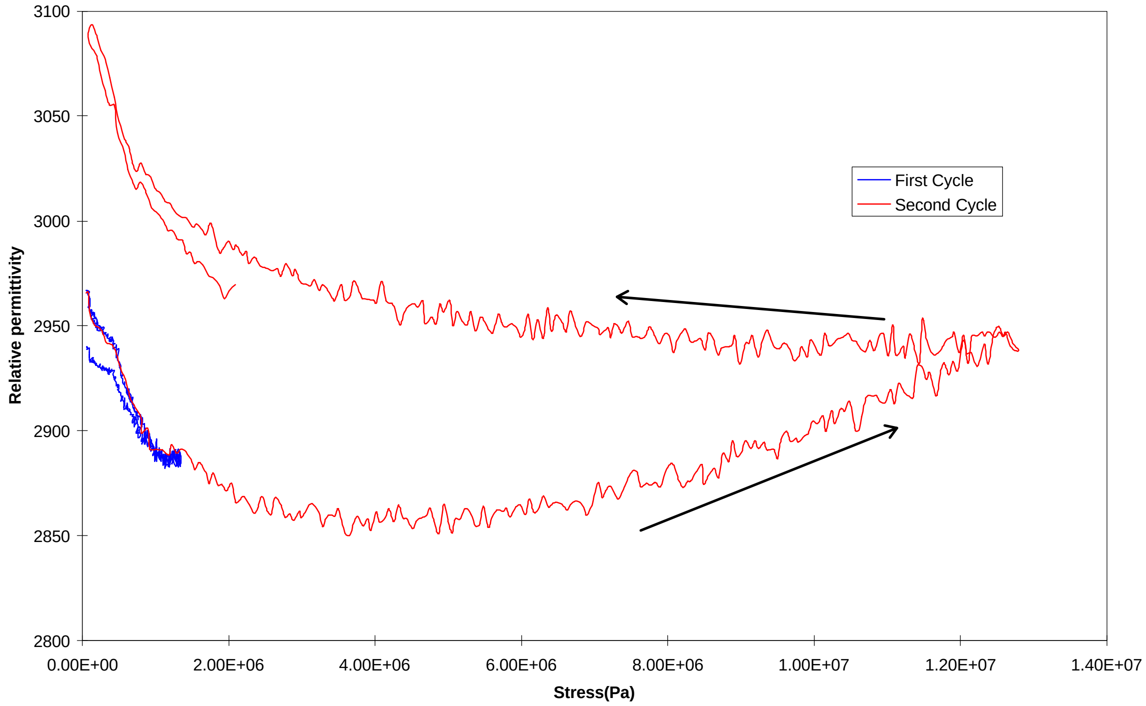

Figure 7: Low field permittivity at 1kHz under an applied axial load for a soft 5H material (sample 5mm long, 10mm diameter).

Electrical stress - effect of static stress on high drive level properties

Polarisation Loop Measurement

For measurements at high drive levels, electrical isolation of the sample from the loading chain and the measurement of displacement needs to be carefully considered. The sample holder is based around two alumina discs 32mm diameter and approximately 8mm thick. Electrical contact to the sample is made by gluing thin copper sheet (0.2mm) to the alumina. The discs also each have a ring of tuffset plastic clamped to them to enable attachments - such as displacement sensors and cable strain relief points - to be connected near the sample. This assembly (Figure 8) was used for the majority of the tests discussed here because of its ability to electrically isolate the sample and transfer the mechanical load effectively. Although materials other than alumina could have been used there is a requirement for the holder to be as stiff as possible in some of the mechanical cycling tests.

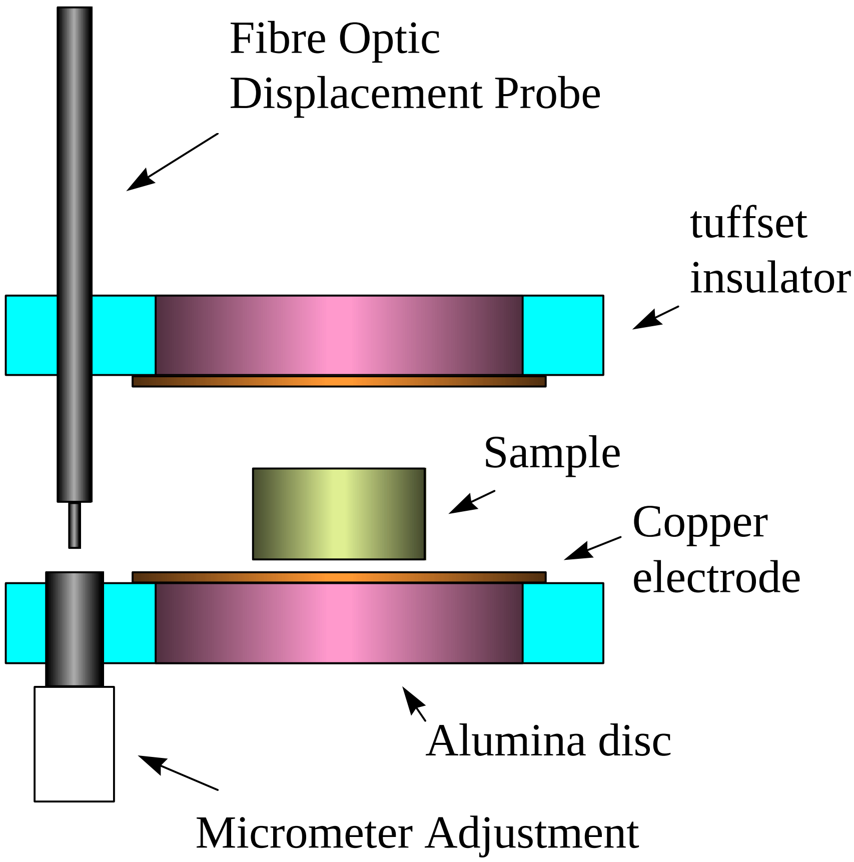

Figure 8: Schematic of sample holding fixture

This complete assembly was placed inside the mechanical loading rig (discussed later) equipped with a manually operated hydraulic actuator. However, almost any mechanical testing machine would have sufficed. This enables the measurement of various piezoelectric parameters under static stresses to be carried out using the measurement methods previously described in NPL report CMMT (A)98.

Initially the measurement of displacement was performed using capacitance sensors attached to the tuffset blocks. However, this method was abandoned because of difficulties due to the small gap between the two grounded guard rings, which are part of the sensor, which caused occasional short circuit paths. Although the capacitance sensors could have been used with an improved design of the sample holder, it was simpler to use an MTI fibre optic displacement measurement probe, (MTI 2000 Fotonic Sensor, MTI Instruments, Latham, NY, USA).

Figure 9 shows simultaneous (a) P-E (polarisation-field) and (b) S-E (strain field) hysteresis loops for a 5mm thick sample 10mm diameter of a soft PC 5H material under static stresses of 0, 6, 12, and 32MPa, with a driving field of 1.1kV/mm peak to peak at a frequency of 1Hz.

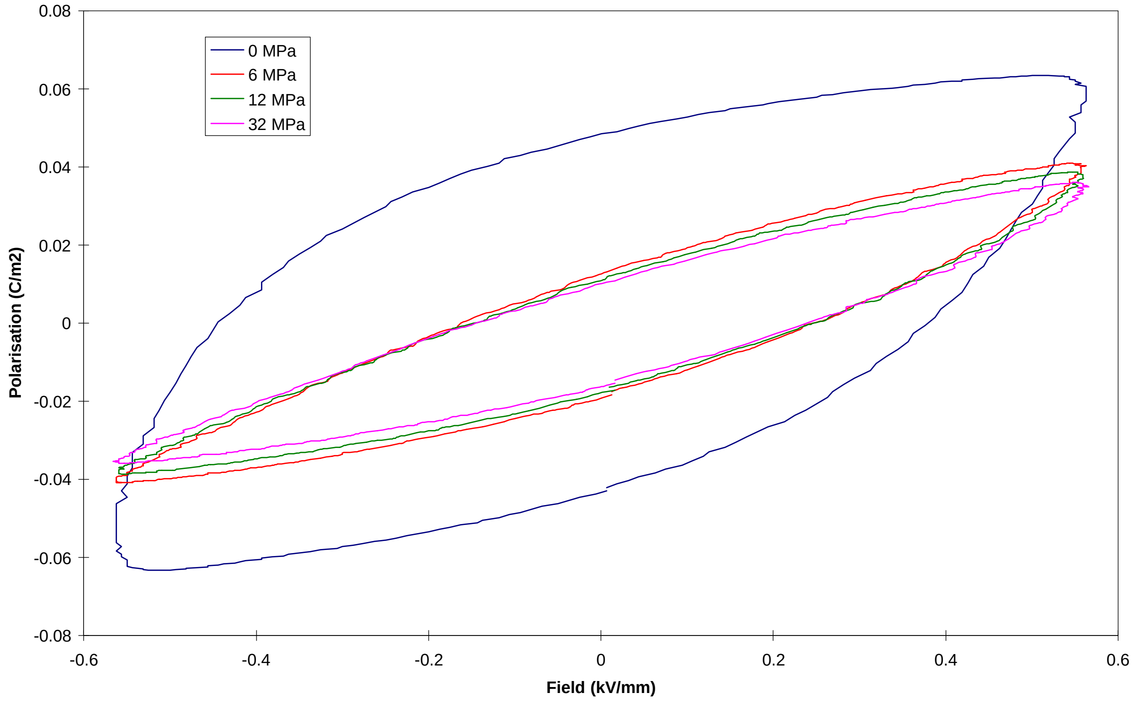

(a)

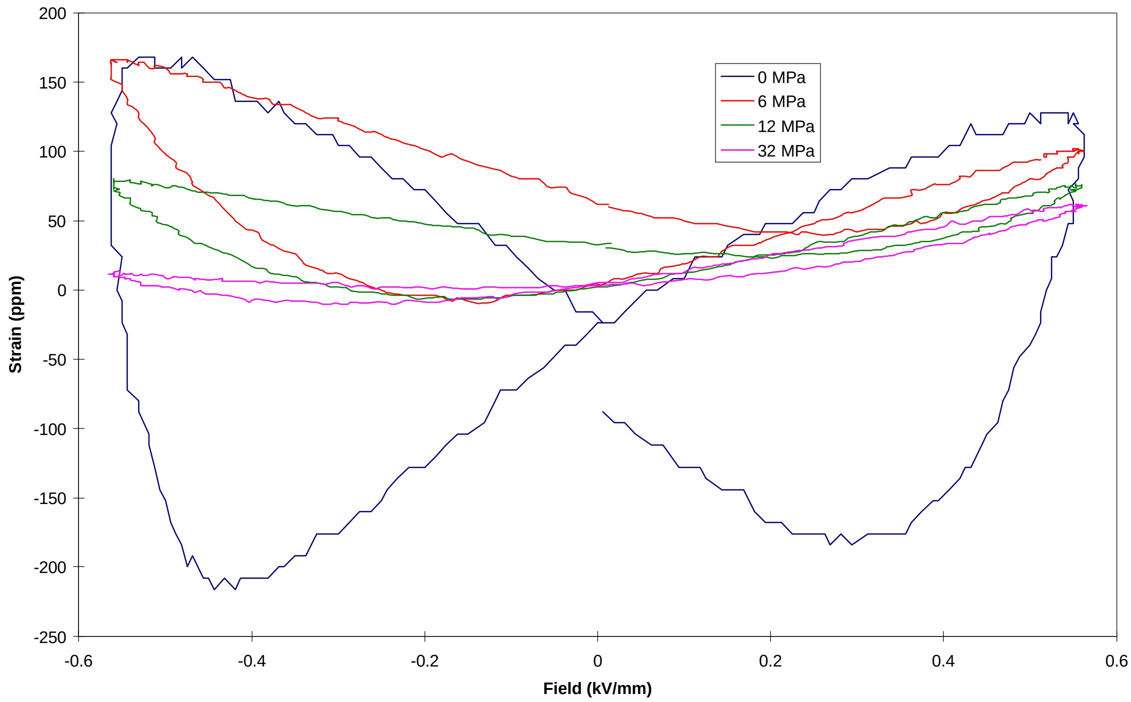

(b)

Figure 9: Simultaneous a)P-E and b)S-E loops for a soft PC5H material, at 1 Hz for axial stresses of 0, 6, 12 and 32MPa. Frequency 1Hz, sample dimensions 5mm long, 10mm diameter.

The method of loading the sample is via a combination of hydraulic actuator to achieve the required static load, and then securing the load via a lock nut. Obviously if the system is very stiff the applied field will generate a stress, rather than a strain in the sample, invalidating the measurement. However for these experiments the 5kN strain gauged load cell used to monitor the load was a relatively compliant component in the system. The effect of field-generated strain on load could be monitored by a change in the load-cell reading as the field was applied. At low values of static load the applied field generated strain was comparable with the movement in the load cell, whereas at higher loads the load cell movement was much greater, and the field-induced displacement was generally reduced. The zero-load measurements were, in fact, carried out at 0.17kN which is the minimum load that could be achieved due to the mass of the sample holding furniture.

From Figure 9 it can be seen for the soft material that both displacement and polarisation decrease with increasing stress. The change in behaviour is non linear with the largest change between the 0 and 6MPa curves. The P-E loops for the 6, 12, and 32MPa stresses are very similar whereas their respective S-E loops are different. This is probably because much of the displacement response results from 90° switching whereas most of the polarisation response is due to 180° domain switching. Although the applied stress will enhance 90° switching, the effect will depend on the sign of the stress. Compressive stresses will enhance 90° switching that leads to a reduction in length, since there is no extra driving force to switch these back

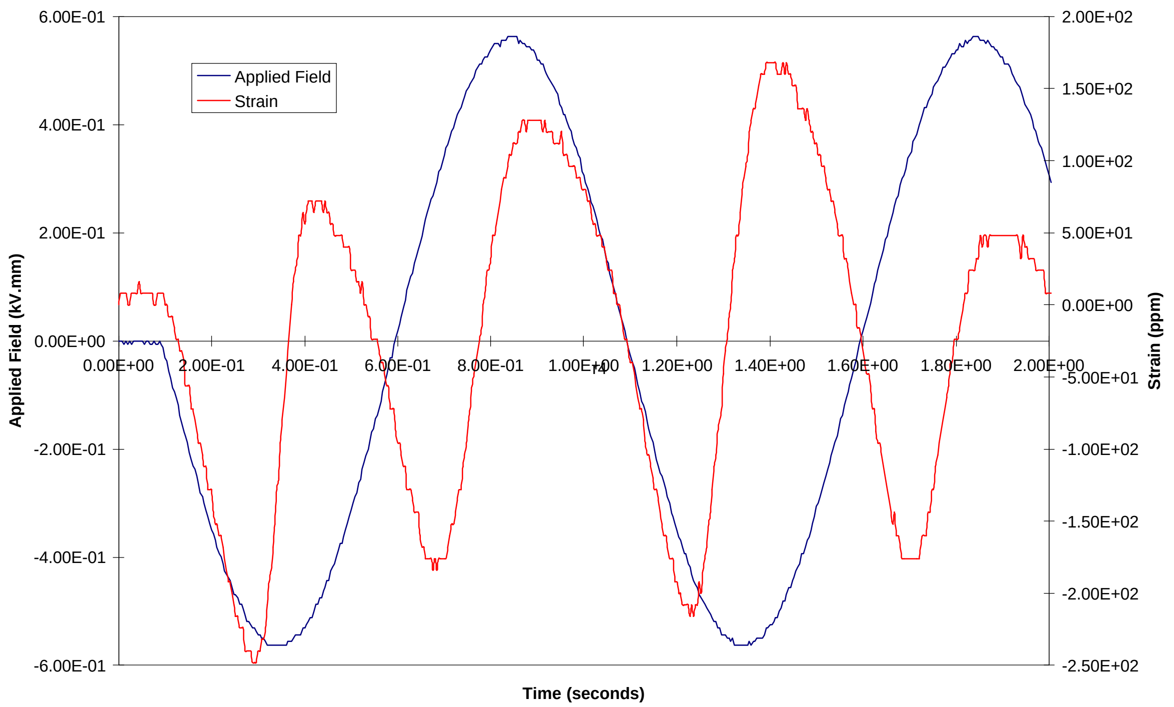

Figure 10: Applied voltage and strain output for the first applied field cycle after releasing the load from 32MPa to zero. Frequency 1Hz, sample dimensions 5mm long, 10mm diameter

until the compressive load is released (Freeman et al. 1996). This effect is most noticeable on the first high field cycle after the imposition or release of a stress. If a compressive load is placed on the sample, the sample contracts under this load under a combination of linear elastic and 90° switching, and the length is stable after some short time. Then when the sample is cycled electrically in the first cycle there is sufficient extra energy for more 90° switches to occur, and there is a further contraction, which is then the new stable length. This strain is only recovered upon release of the stress, and this recovery is aided by application of an electric field of opposite polarity. This manifests itself in displacement-time curves where the sinusoidal displacement drifts over the first few cycles until a stable strain is achieved (Figure 10).

Because of some perceived problems related to the positioning of the fibre optic probe it was decided to verify the fibre optic displacement measurements using strain gauges attached directly to the piezoceramic. The fibre optic probe effectively measured the displacement of the two alumina platens, and it was thought possible that at low loads the sample might not be in intimate contact with these. In order to capture the signal from both strain gauge and fibre optic probe the current signal on the data capture system was replaced by the strain gauge amplifier output. To accommodate the strain gauge on the sample the length was increased to 10mm. The strain gauge was a single gauge measuring the displacement in the polar direction, used in a quarter bridge set-up. The strain gauge signal was calibrated by comparison against the fibre optic probe measurements at high loads when it was certain the alumina platens were in contact with the sample. In fact there was very little difference between the fibre optic and the strain gauge signal. The strain gauge system had the added advantage that it was possible to determine the *elastic offset* caused by the application of a static load, which was not possible to determine using the fibre optic probe having an insufficient measuring range.

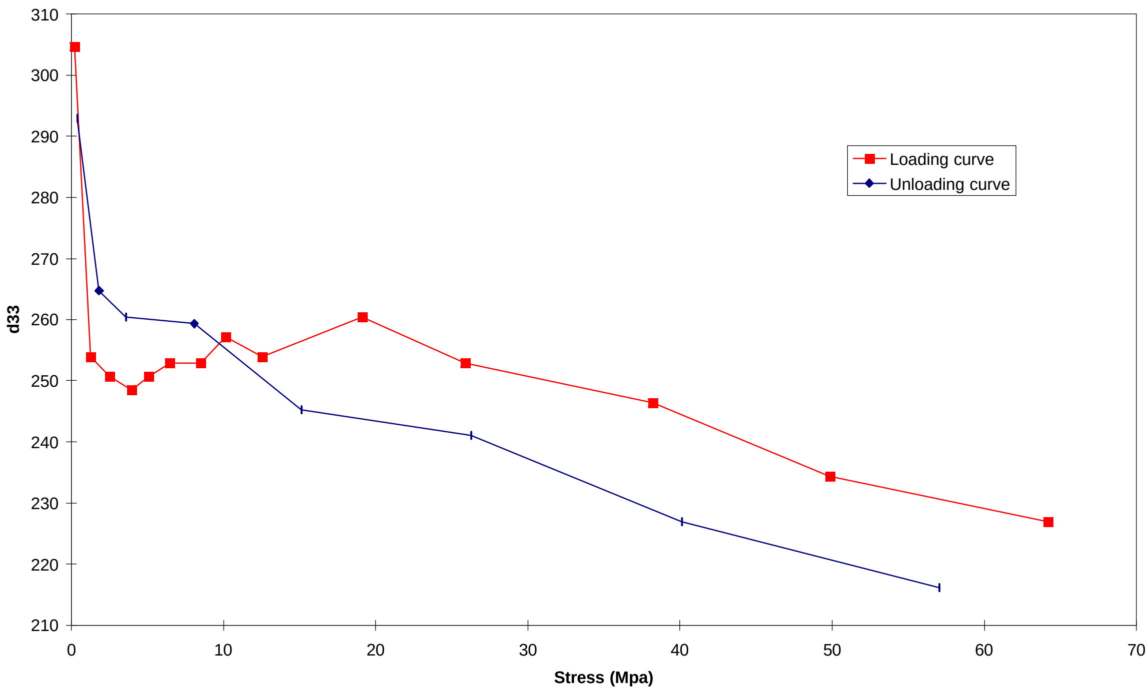

Figure 11: d_{33} against applied axial stress for a 10mm thick 10mm diameter hard PC4D sample, for loading and for unloading.

Figure 11 shows a curve of the strain gauge measured d_{33} against axial load for a 10mm diameter, 10mm long PC 4D piezoceramic. There are two curves; one for application of the load and one for removal of the load after leaving overnight to stabilise at maximum load. It can be seen that the behaviour is hysteretic and that there is a large discontinuity at very low loads. The trend for the curve is downwards i.e. less displacement at increasing axial load, and although this is intuitively what is expected, this conflicts with previous studies on hard ceramics. Krueger found low field d_{33} increased with increasing load (Krueger, 1967), and Hennig found high field displacement of thin stacked actuators increased to a peak at around 30MPa (Hennig et al. 1996). However, in a related study (Pertsch et al, 1996) no change in displacement output with increasing load was observed for a hard composition of dimension 10mm diameter by 8.8 mm. As noted by others (Krueger, 1967), it is probable that mechanical clamping in thin disc shapes leads to a completely different stress pattern compared to those in long cylinder shapes.

The stress strain behaviour of the material was also monitored with the attached strain gauge, and the results shown in Figure 12. Again this curve conflicts with most studies of deformation for hard materials (Figure 1), where a linear stress-strain is expected until close to a stress of 100MPa when the depoling leads to a softening of the material (Cao et al. 1993). In this study

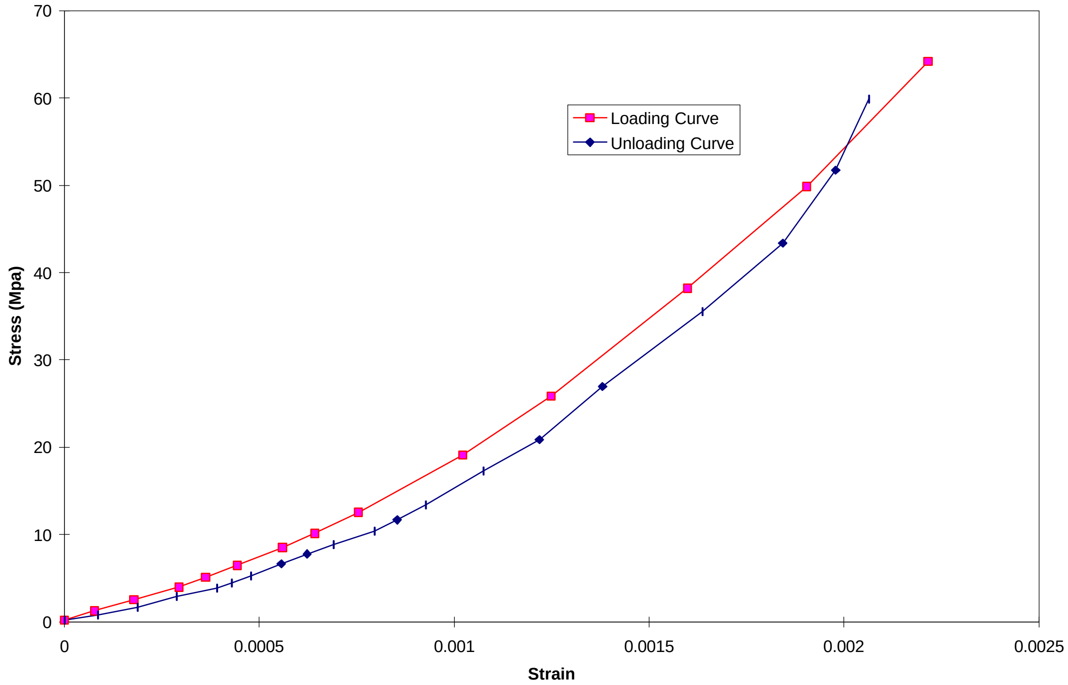

Figure 12: Stress strain curve for sample in Figure 11

the material seems to get stiffer as load increases. Although this could be due to mechanical bedding-in of the system, the unloading curve is similar and subsequent cycles reproduced this curve. It must be noted that the experiment is not purely stress-strain, since, at each point on the curve, the sample had a large cyclic electric field applied to it. It remains to be investigated if this leads to a different stress-strain curve.

Impedance Spectroscopy

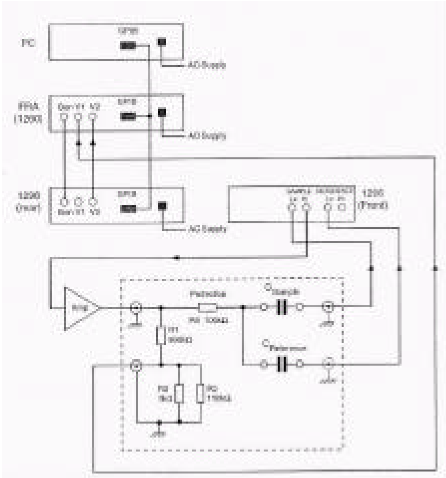

Figure 13: ***High voltage dielectric interface measuring equipment for electrical fatigue measurements***

As described in NPL report CMMT A(98), permittivity and loss are measured using an impedance analyser and associated high sensitivity dielectric interface unit. This system, is able to automatically measure the dielectric current, voltage and phase across the sample and compare this to the identical drive through either an internal or (in this case) an external standard reference capacitor.

In the experiments described in this report, the external standard reference capacitor had been chosen to have an absolute value of capacitance similar to the samples being tested and has traceable values of capacitance and loss which is independent of field and frequency. The details of the high voltage stress circuitry is shown in Figure 13. The reference measurement is used to eliminate the effects of extraneous capacitance and loss, since the absolute values of phase (tan delta) which are measured will be affected by the connection cables and interfaces. Additionally, corrections for phase shifts introduced by the high voltage amplifier will need to be made for measurements to be made at high voltage.

The TREK RT6000HVA is the high voltage amplifier used in all these measurements for control of output voltages in the range 0 - ± 4kV with an output current of 0 - ± 20mA peak. It is configured as a non-inverting amplifier with a voltage gain of 1000 V/V. It has a solid-state four-quadrant, active output stage which sinks or sources current into reactive or resistive loads. The RT6000HVA is short circuit and overload protected and supplies a precision voltage monitor output which provides a low-voltage replica (in terms of voltage and phase) of the high voltage output. It has a small signal bandwidth of DC to 1kHz (-3dB) and a large signal bandwidth of DC to 200Hz. The DC gain accuracy is better than 0.1% over its full range.

A series of measurements were made on samples of PZT materials of various thickness. The samples were all electroded and poled.

Resonance determination of experimental system

The complete measurement system is a complex mechanical system comprising;

- the piezoelectric sample
- its connections
- electrical and insulating spacers
- steel rams and locating rings
- load cell mounts and internal construction
- fatigue rig bolts and overall frame design
- hydraulic or otherwise static loading chain
- cyclic actuation device (piezoelectric actuator for example)

This linear mechanical system may introduce various frequency anomalies and resonances which would affect the measurement results and thus the apparent response obtained from the material under test. Thus, before carrying out any fatigue testing, it was important to determine the frequency response of the system without the sample in place (substituted by a linear ceramic of similar stiffness and modulus) and thence with the sample in place. The electrical or mechanical loading, with the sample in place, in these series of preliminary experiments, were kept to a minimum in order to minimise property change before the main fatigue experiments were initiated.

The dispersion graphs, Figure 15 and Figure 14, clearly demonstrate that resonance takes place at different frequencies dependent on loading, material type and other experimental artefacts.

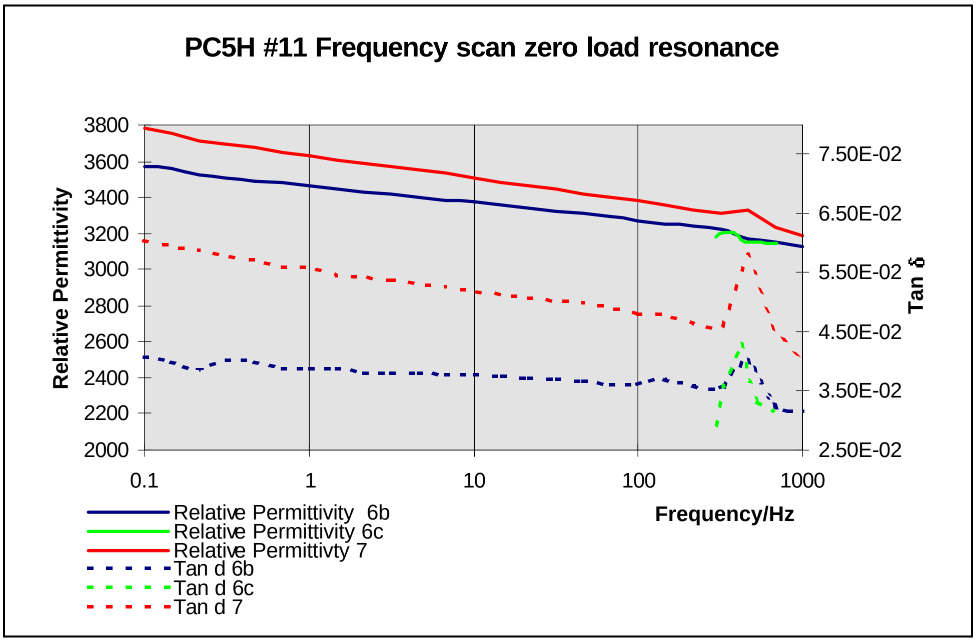

Figure 15: Resonance scan for soft material in E-Rig fatiguing system

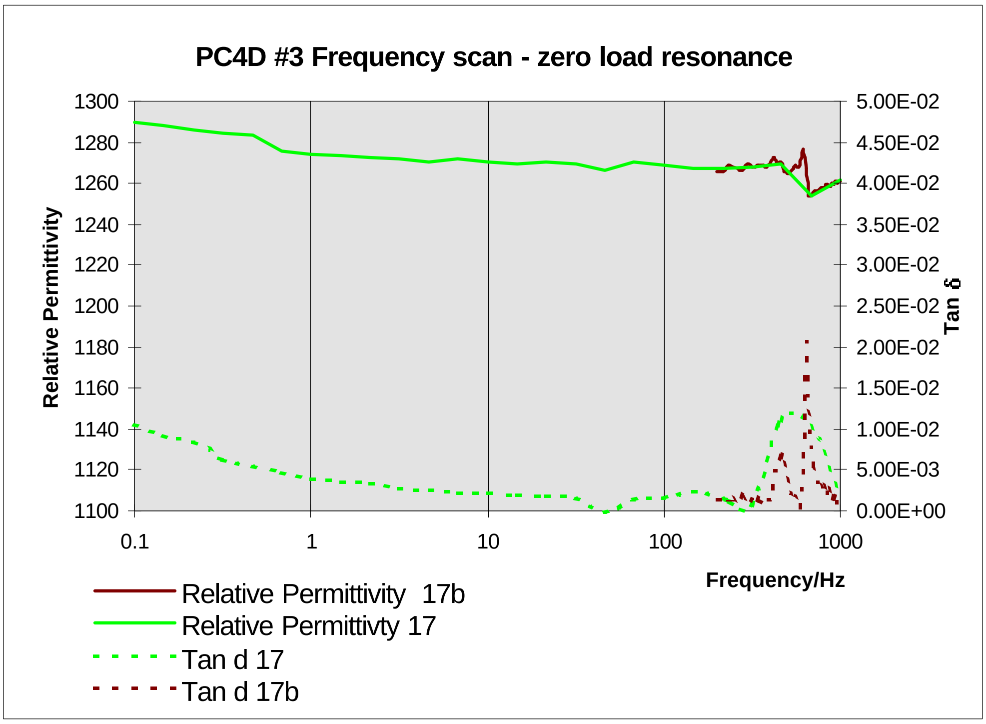

Figure 14: Resonance scan for hard material in E-Rig fatiguing system

Resonance behaviour in the test system can be clearly seen in the dielectric loss measurements, and also to a lesser degree in the permittivity results.
To avoid difficulties in interpretation of results, the measurements should be conducted well away from the resonance frequencies, and for this reason the frequency used in the electrical and mechanical fatigue experiments were made at 100Hz.

Static Mechanical Loading - Dielectric Property Measurements

The effects of electrical field on the measurements of permittivity and dielectric loss tangent have been previously described and reported in the literature (CMMT (A)98, Audigier et al. 1994, Hall 1998, Li et al. Robels at al., Wu et al., Sherrit et al. 1997). The increase in permittivity and dielectric loss has been attributed to an increase in the extrinsic ferroelectric domain wall motion and domain switching at high applied fields. The relative contributions arising from reversible domain wall motion and that arising from domain switching has been the subject of a recent paper (Hall 1998). One goal of the present work was to develop suitable experimental measurement methods which enables effects such as increasing the magnitude of cyclic applied electric field and static mechanical loading on the dielectric properties of PZT materials to be determined. Static mechanical loads, generated using a hydraulic ram set within

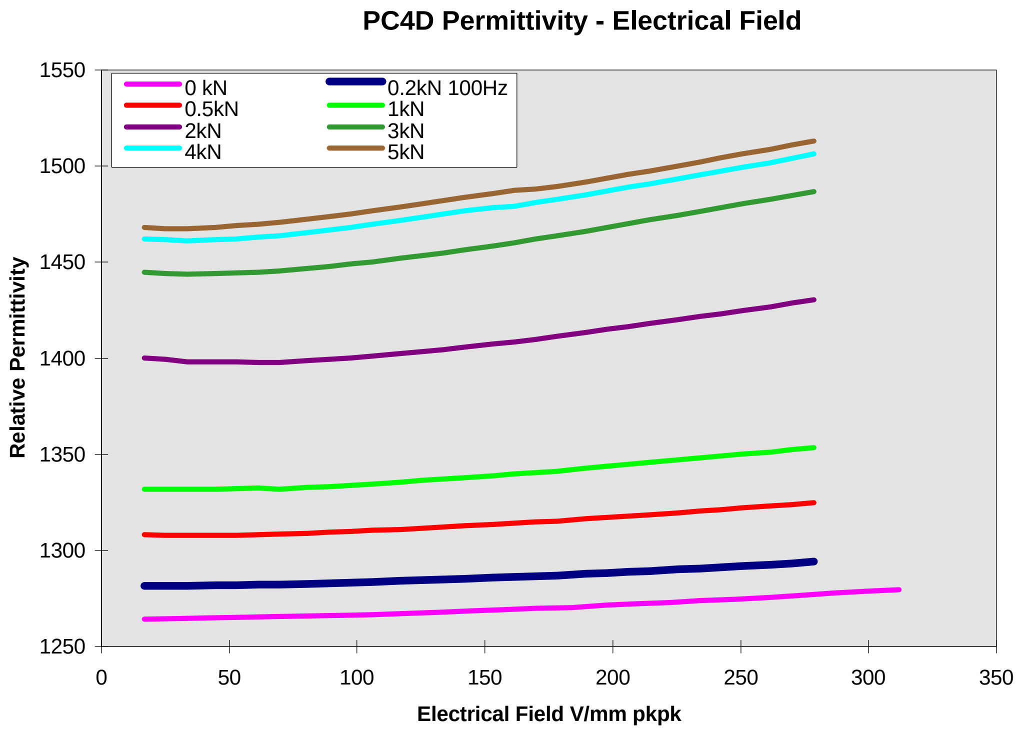

Figure 16: ***Permittivity as a function of static load and electrical field for PC4D hard material at a frequency of 100Hz***

the 'Plint rig', described later, were applied to the materials under test. The measurement method described in CMMT(A)99 ramped the applied electric field from a low signal response to values reaching approximately 300V/mm pk/pk. This value should be well below that necessary for domain switching. The graphs in Figure 16 and Figure 17 demonstrate the change in permittivity and loss for a hard material PC4D as a function of applied electric field and at various uniaxial static loads.

The data for the PC4D material shows a large increase in permittivity with increasing uniaxial stress (approx. 16% for low signal response) and similarly a gradual increase in permittivity with electrical drive, as expected. The increase in permittivity with static stress has been demonstrated elsewhere for these types of piezoelectric materials (Audigier et al. 1994, Sherrit et al. 1997, Meeks 1975). In a similar fashion, the loss tangent increases with increasing

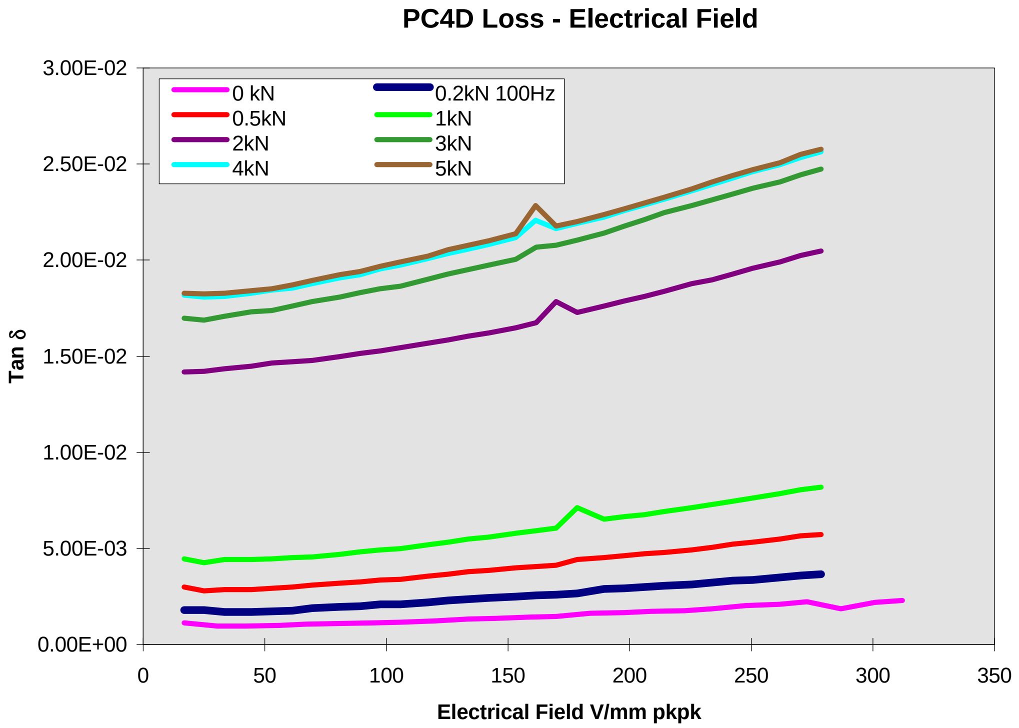

Figure 17: Loss tangent for PC4D hard material showing increase with electric field and increase with static loading.

electric field and static stress, Figure 17.

Exposure to high driving fields or static stresses will always act to increase tanδ, (Krueger 1967, Meeks 1975). The samples diameter to thickness ratio of 1:1 (10mm diameter and 10mm in thickness) and the presence of high friction interfaces between sample and uniaxial stress platens are likely to have introduced residual lateral clamping at the ends of the sample. This would have the effect of reducing the changes in permittivity with increasing stress (Krueger 1967). It is important to minimise any residual clamping at the ends of the sample which may be accomplished through the use of polished end pieces, polished sample ends and the use of a lubricant such as graphite powder applied between the mating surfaces. It is additionally important to ensure that the stress state present within the sample is as uniform as possible. This may be accomplished by ensuring that the diameter to thickness ratio exceeds 3:1 (Audigier et al. 1994, Berlincourt 1959).

The data obtained for the soft 5H material differs markedly from the results obtained with the harder material. In this case, the permittivity and loss tangent decrease with increasing static stress, whilst still increasing with applied electric field, Figure 19 and Figure 18.

The increase in dielectric properties with increasing electric field is expected and has been

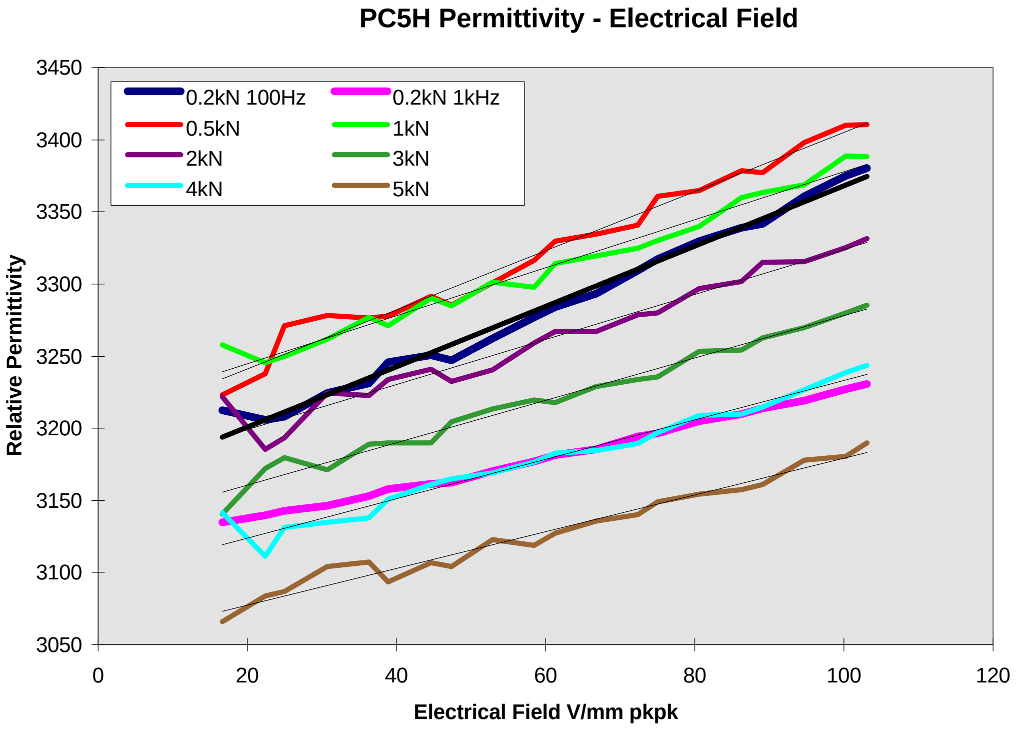

Figure 19: permittivity as a function of static load and electrical field for PC5H soft material

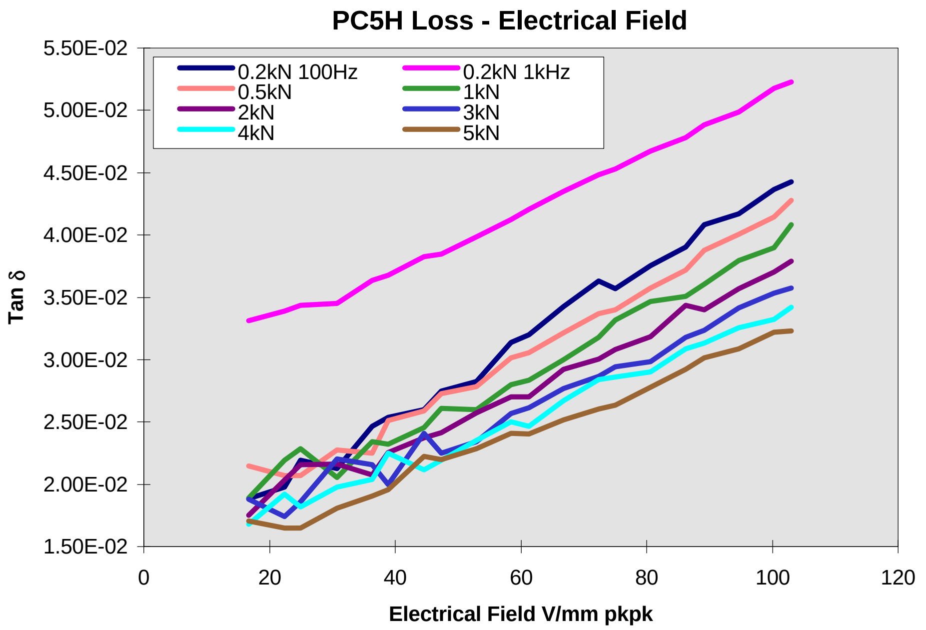

Figure 18: Loss tangent for PC5H soft material showing increase with electric field and decrease with static loading.

widely reported, as having similar origins to the hard materials response, and linked to the irreversible domain wall motions (see Hall 1998). The effect of applying a static uniaxial mechanical stress field to soft materials has shown (Audigier 1994, Kruger 1967, Meeks 1975) that with increasing static stress a gradual decrease in loss tangent and permittivity are observed. The values of permittivity and loss were additionally shown to increase with increasing electric field, as observed in this work. It may be that with the softer materials stress clamping acts to hinder the generation of new domain walls which otherwise would have contributed to the permittivity and loss, evident in the harder materials (Krueger 1967). However, it is still not clear why the stress dependence of the dielectric properties of hard materials differ so dramatically compared with soft materials.

Electrical fatigue - Dielectric Property Measurements

Electrical fatigue for hard and soft materials was measured using dielectric impedance methods, described above and previously (CMMT(A)98, (A)99). The parameter used to monitor the degradation in properties of the material with time was its permittivity and dielectric loss tangent. The sample was set up within the 'Plint' rig - described later - and a static preload of 5kN was applied. The permittivity and loss were measured as a function of time for a relatively short duration of approximately 10^4 cycles at an applied electric field of 500V pk/pk/mm at a frequency of 100Hz. Electrical fatigue in piezoelectric ceramics is manifest as a degradation in polarisation and a corresponding increase in loss (see Chen et al. 1997 for detailed references to fatigue in ferroelectric thin/thick films).

The degradation of dielectric properties with electrical cycling of a soft PC5H material is shown in Figure *20*a. and for a hard PC4D material in Figure 20b. It is clear that a loss in permittivity and a corresponding increase in loss is observed at fatigue times of order 10^3 cycles for the hard material and approximately 10^2 cycles for the soft material. After 10^4 cycles the permittivity for the hard material and soft material had both degraded by approximately 0.8% of its initial value. The corresponding increase in loss was approximately 2.5% for the soft material, and 20% for the hard material. The hard material clearly exhibited a higher degree of degradation if the degradation is described as a percentage change in loss. However, the results presented in this report, are tentative and further analysis will not be carried out till further data sets are recorded.

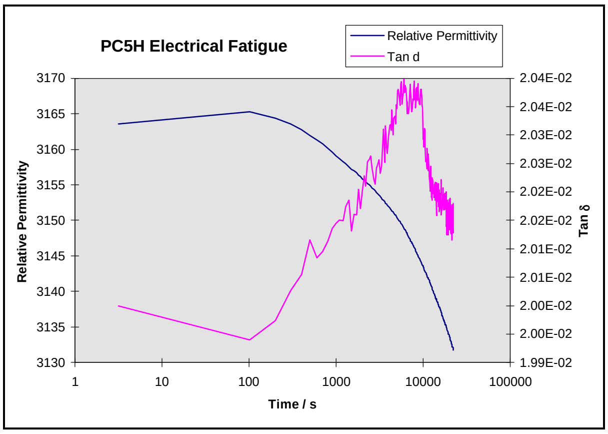

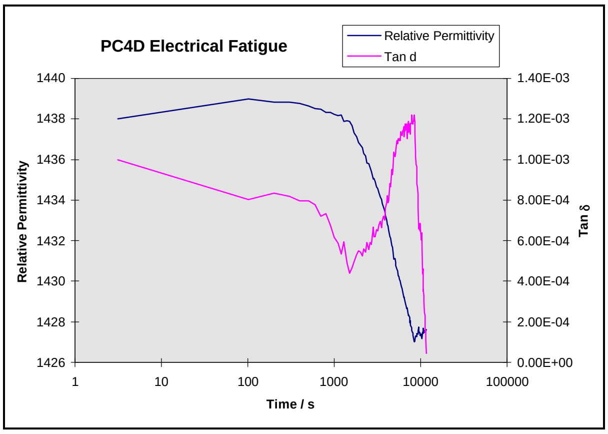

Figure 20 (a): Electrical Fatigue for PC5H ***(b): Electrical Fatigue for PC4D***

Mechanical fatigue: High stress rate Measurements

So that mechanical cycling experiments can be made at high stress rates, several methods for generating mechanical stress were investigated. The need for measurements to be conducted under high stress rate is two-fold; firstly the material may behave differently at higher stress rates due to inertia associated with domain wall mobility; and secondly in order to carry out degradation experiments over many decades of cycles it is obviously more convenient at higher frequencies.

The frequency limit for conventional screw thread driven mechanical testing machines is around 1 Hz and this can be extended to around 100Hz using hydraulic actuators. To extend the testing regime further it was decided examine the use of a magnetostrictive and a piezoelectric actuator. In order for these actuators to be used in a stress generating mode they must be confined within a stiff loading frame to ensure that as much of the displacement generation results in stress in the device-under-test and not in expansion of the loading frame.

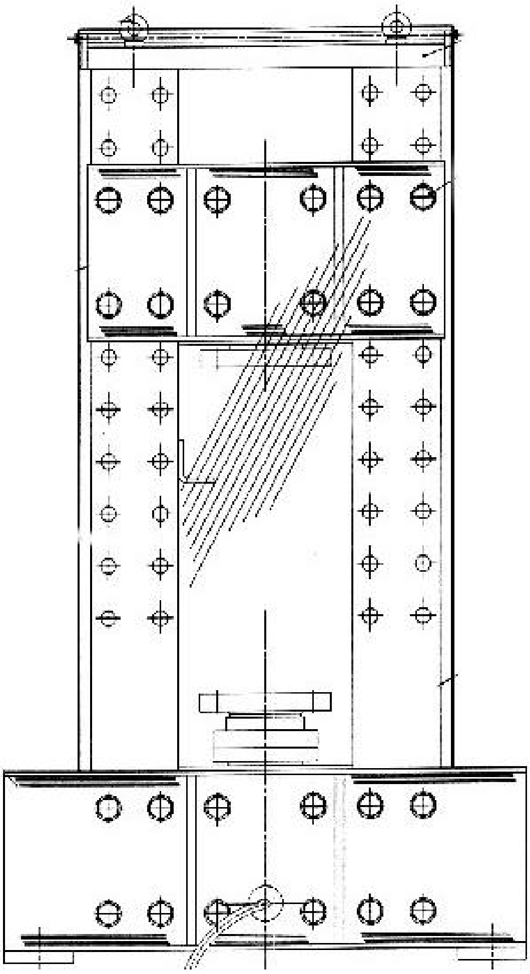

Figure 21: Engineering drawing of stiff loading rig.

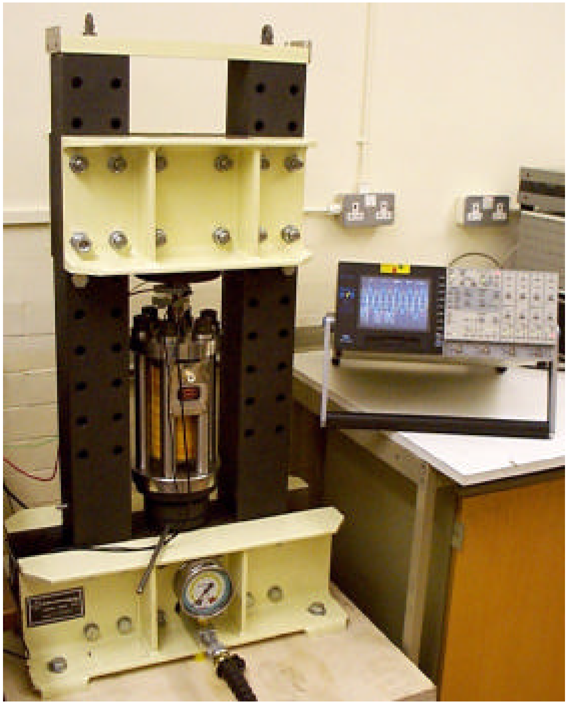

Figure 22: Photograph of Plint rig and magnetostrictive actuator set up for fatigue measurements

The magnetostrictive actuator is 315mm long with a diameter of 170mm and a maximum stroke of 100 microns, whilst the piezo actuator is 65mm long with a 50mm diameter and has a maximum stroke of 20 microns. A stiff frame was designed to accommodate either of the actuators. Because of the very different size and displacement output of the actuators the frame was in fact larger than it needed to be if only one of the actuators was used. Figure 21 gives a engineering drawing of this loading frame, and Figure 22 a photograph of the rig with the magnetostrictive actuator set up for mechanical degradation measurements.

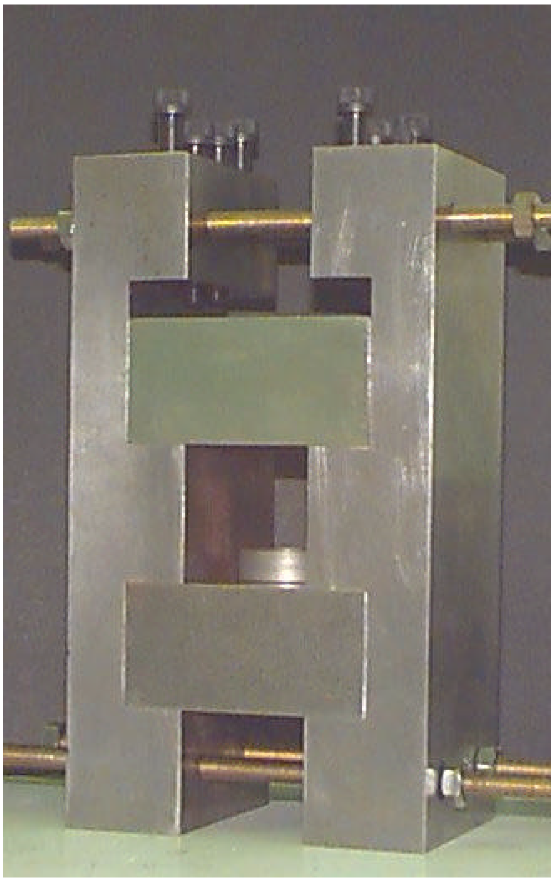

Figure 23: Photograph of E-rig.

A second stiffer and more cost effective test frame was designed to accommodate solely the piezoelectric actuator. This frame (Figure 23) termed the ‘E-rig’ is fashioned out of two vertical E shaped members, and two horizontal members locate in the slots in the E members. All the members are made from 100mm by 50mm stock and the static loading is achieved by 8 M10 bolts at the top.

Using the magnetostricitve actuator sinusoidal loads of around 2 kN peak to peak at around 150Hz are possible, and with the piezoelectric actuator loads of up to 9kN peak to peak at 10 Hz, but at 100Hz this is reduced to 1 or 2 kN. For both actuators the major limiting factor controlling high frequency loading is the power output of the drive electronics, and it is likely that the actuators could achieve higher frequency output given more powerful drive electronics. For the piezoelectric actuator the capacitance of the actuator of about 0.7μF limits the maximum frequency to around 10Hz using a TREK 50/750, with a maximum peak current of 100mA at 0-1500volts. It is possible to get large mechanical outputs in the kHz range if the actuator is driven at resonance, but it is not clear how stable the mechanical forces generated at resonance will be. The actuator may need some form of feedback to maintain resonance instead of using a linear drive input. Also at these frequencies it would be difficult to get information over the first 5 decades of cycles as this occurs too quickly.

Mechanical fatigue - measurement of d_{33}

Actuator manufacturers utilising piezoelectric materials routinely need to have reliable data on both d_{33} and Young’s modulus (Y^E_{33}) (as well as linearity and hysteresis). d_{33} is an extremely important parameter since it dictates the extension per unit applied field that the manufacturer can realise from many practical actuators. It is expected that parameters such as sample thickness, sample geometry, electrode area and shape, electric field strength and mechanical stress methods of application, intensity and frequency will have some impact on the measured value of d_{33}.

The measurement of d_{33} is normally made by measuring the charge developed across the surfaces of a sample during AC mechanical loading. The charge developed must be measured in a closed circuit condition (shorted) such that charge does not accumulate on the surfaces of the sample. d_{33} can be calculated as the ratio of the charge to the mechanical stress. An alternative calculation measures the strain (or extension) developed during the application of a driving field. The ratio of strain to applied electric field similarly equates to d_{33}. This latter method is preferred for actuator manufacturers.

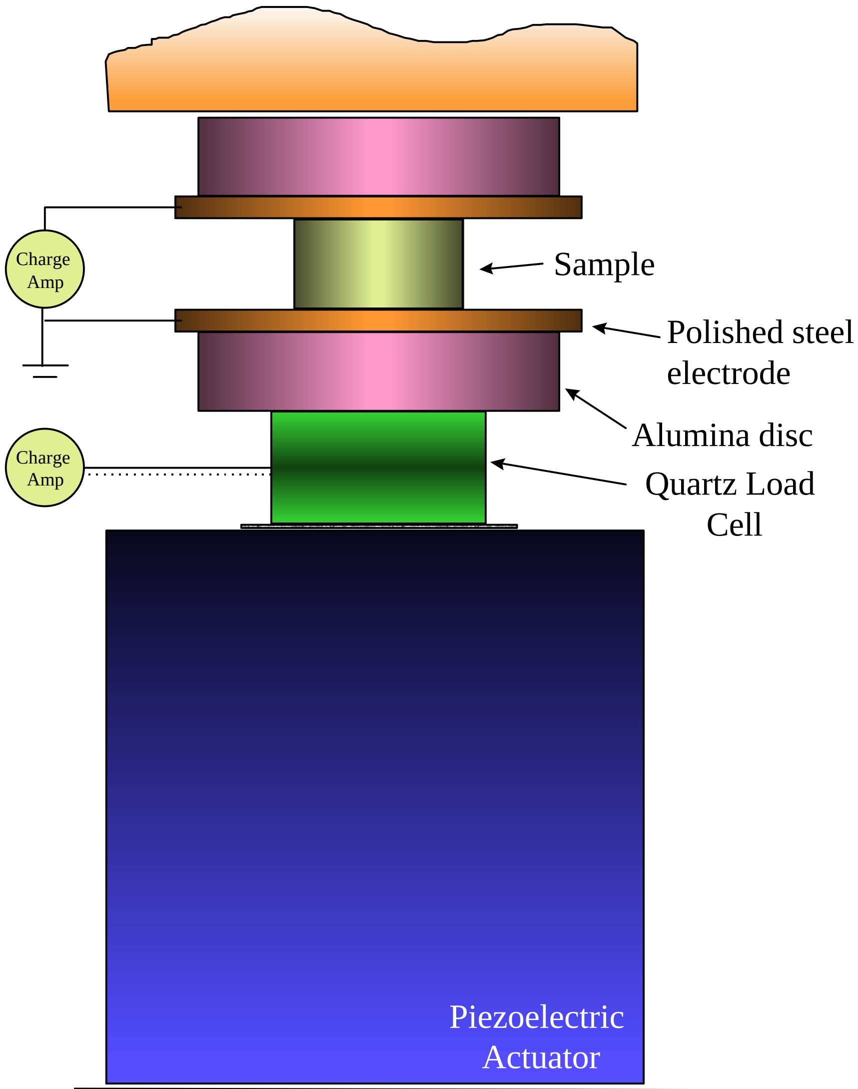

Figure 24: Schematic set up for the measurement of d33.

In these measurements the piezoelectric charge coefficient was measured using the direct method - vis. charge collected on the surface of the piezo element with applied mechanical cyclic loading. The experimental set up is shown in Figure 24. The cyclic mechanical stressing was accomplished using the piezoelectric stacked actuator used in previous experiments. The cyclic force was monitored using a quartz load cell, and the charge generated collected using polished metal contactors above and below the sample. Charge amplifiers operating in virtual earth mode collected this charge. The force and charge results were digitised and collected using standard ADC techniques and the experiment was controlled and monitored using LabView software. Mechanical fatigue may be measured using this equipment by applying a varying AC force using the stacked piezo actuator, and a static force using the screw adjusters. A static DC force of 18MPa was applied to the sample so that previous work might be compared with these experiments (Damjanovic (a)1996, (b)1996, (a)1997, (b)1997). This method of measurement has been applied by others and has been shown to be valid for the assessment of d_{33} (Audigier 1994, Damjanovic (b)1996).

The logarithmic dispersive relationships for soft materials have been described using the Rayleigh law originally discovered to describe the magnetic permeability in ferromagnetic materials (Damjanovic (b)1996, (a)1997). In a series of experiments conducted at NPL, the logarithmic dependence of d_{33} on frequency for soft materials has been demonstrated and confirms the data generated by the group at Lausanne (see references to Damjanovic). The results are shown in Figure 25. The piezoelectric coefficient, d_{33}, decreases with the log of frequency, as expected for soft materials. The data plotted for PC4D hard material does not exhibit the dispersive relationship that is found for the soft materials. This indicates that domain wall pinning (the phenomenon that the Rayleigh law attempts to describe) is not occurring in the hard materials. This is consistent with current thought. A static prestress of 18MPa and a cycling AC load of 3MPa was applied.

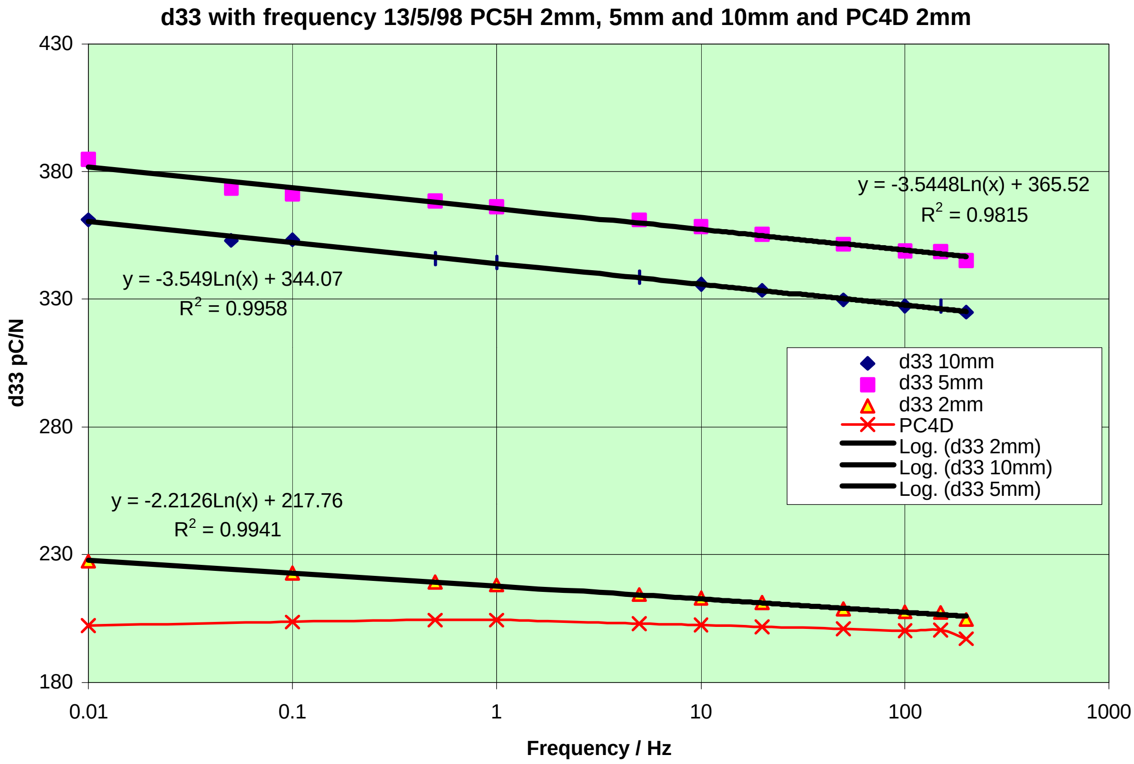

Figure 25: Piezoelectric coefficient measured using the E-rig system previously described.

An interesting observation is the dependence of d_{33} on sample thickness, Figure 25, with the values lowest for samples of small thickness (2mm), an intermediate value for the 10mm samples, and the highest d_{33} values for the intermediate 5mm thickness. A similar anomaly has previously been observed at NPL for permittivity and polarisation measurements on the same materials. Possible explanations may include the reduced poled strength for the 10mm sample arising from insufficient high tension capability of the manufacturers poling equipment and the possibility of non-uniform stress gradients within the thinner samples and edge effects arising from reduced surface constraints and surface friction between sample and rig. Attempts to determine the inconsistencies and anomalous results are being conducted in separate programmes at NPL.

The results in Figure 25 are in agreement with those obtained elsewhere (Damjanovic (a, b) 1997). The piezoelectric coefficient, measured as a function of applied AC stress is shown in Figure 26. At these low pressures (although the static DC pressure was maintained at 18MPa), it is apparent that the domain wall contributions to the direct piezoelectric effect can be readily described by the Rayleigh law (Damjanovic (b) 1996) since the form of the relationship is linear to a first approximation.

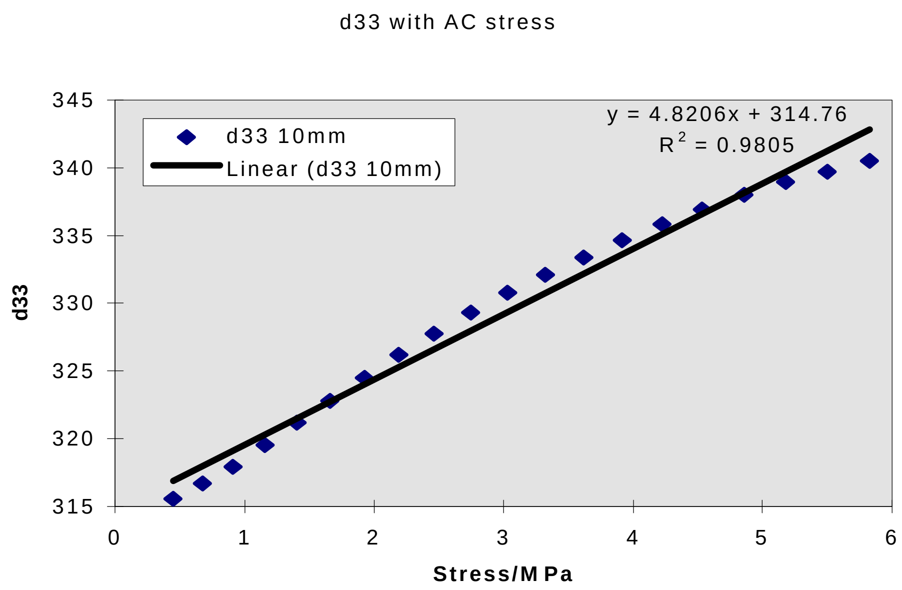

Figure 26: Piezoelectric coefficient, d_{33} with amplitude (pk/pk) of ac pressure.

Mechanical fatigue of PC5H was measured using the E-frame d_{33} rig. The piezoelectric charge coefficient was measured as a function of cycles of the AC force - fixed at 3MPa and 200Hz - and at a fixed DC static preload of 18MPa. The static DC preload was measured using the 'long' integration time constant mode of the Kistler charge amplifiers, and an oscilloscope operated in DC mode. As load was applied the DC preload swing was readily measured on the

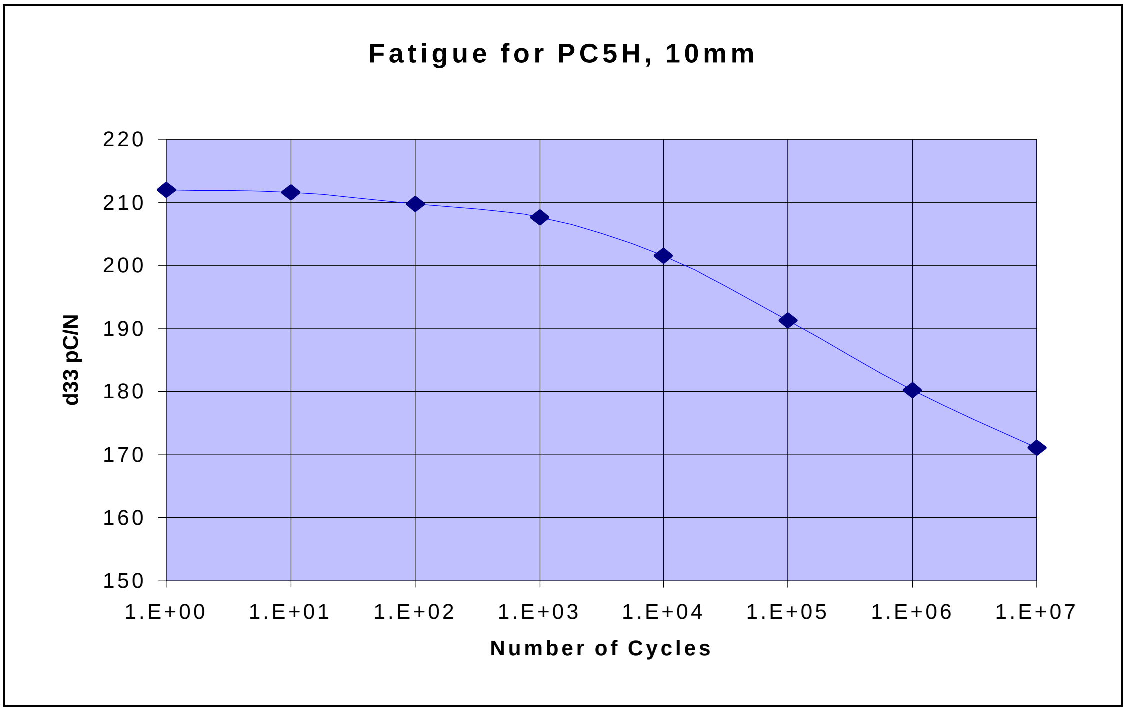

Figure 27: Mechanical Fatigue for soft PC5H measured via d_{33}.

scope trace as a corresponding voltage change. If the quartz load cell and cabling is clean then charge leakage is small enough such that quasi-static measurements can be made using these types of load cell. Once the DC pre-load has been applied, the system may be reconnected and the d_{33} measurements may commence. The data in Figure 27, demonstrates the degradation in d_{33} for a soft PC5H material over a time interval of approximately 10^7 cycles. This degradation amounts to some 20% drop in initial value. This measurement method is clearly quite sensitive to changes in property with time and cyclic stress.

Degradation measurements were also carried out in the Plint rig using the magnetostrictive actuator. The measurements were performed on a 10mm long 10mm diameter PC4D sample which had been used in some previous experiments and had a strain gauge attached. Charge was measured in the same manner as for the E-rig experiments. The load, charge and strain outputs were measured using a DSO with in-built analysis functions, enabling the peak to peak of the waveform to be recorded at suitable times. The frequency was set to 100Hz and the applied cyclic mechanical load was 1kN, and data points were collected every 10 minutes (60000cycles). The normalised d_{33} measurements for 11 days of readings are shown in Figure 28. There is little change in performance, and it is clear that to be able to assess degradation the signal to noise of the present system needs to be improved. Two problem areas were identified, some magnetic pickup on the strain gauge signal from the magnetostrictive actuator, and noise on the magnetostrictive load generation. The load generation was improved by driving the magnetostricitve actuator with an external signal source, however there was still some beating, and also a general drift (over the 11 days) of around 10%. Figure 28 also shows a second shorter run (collecting data every minute) on the same sample with the improved load generation. There is still a lot of noise, and also digitisation error present in the results. The data collection can be improved by using more sophisticated noise reduction such as a lock in amplifier, however the apparent rapid degradation during the second run needs to be investigated. It may be that the temperature of the system and the sample is changing as the magnetostrictive actuator reaches thermal equilibrium. This could also be a reason for the drift in the load generation of the magnetostrictive.

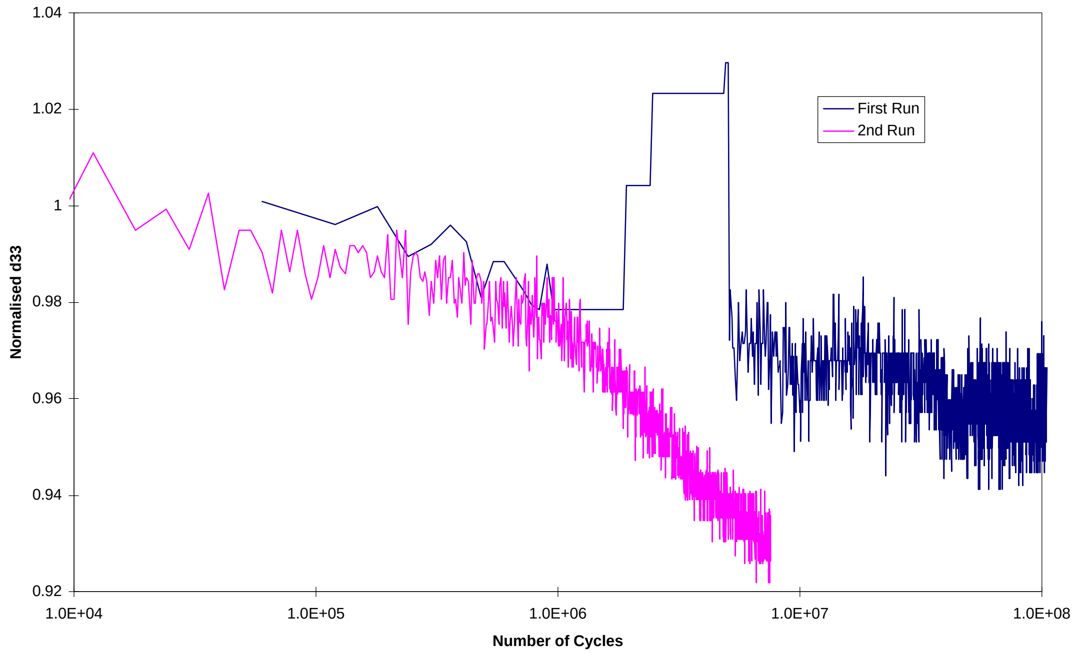

Figure 28: Mechanical fatigue using Plint system and magnetostrictive actuator

Conclusions

Measurement methods developed in the CAM7 project have been extended for the assessment of degradation under high mechanical and electrical cyclic stresses.
In summary:

- High mechanical stresses can depolarise the materials, after only a small number of cycles.
- Measurement of capacitance and loss can indicate degradation in hard and soft materials.
- Sample geometry imposes significant experimental difficulties. Interpretation and comparison of results between samples of various thickness and aspect ratio remains an ongoing problem.
- The effect of mechanical and electrical cyclic stressing on dielectric properties differs for soft and hard materials. This effect has not yet been adequately explained.
- High electrical drive imposes additional complications when measuring and assessing degradation.
- Measurement of strain has been achieved using capacitative techniques, fibre optic probes and strain gauging. All techniques yield similar results, although great care must be taken in assessing the effects of measuring strain ‘off-axis’ with compliant extension supports.
- Polarisation loop and dielectric spectroscopy have both been shown to measure the cyclic degradation of PZT under load.
- Equipment/sample resonance must be identified and either eliminated or measurements should be made well away from the characteristic frequencies.
- Electrical and mechanical fatigue has been measured for soft and hard materials. Preliminary results indicate a loss in permittivity, an increase in loss and a decrease in d_{33} with number of cycles.

This report represents the work conducted in milestone 4 of CAM7, a DTI project on the Characterisation of Advanced Materials, ‘Electroactive materials properties under conditions of high stress or stress rate’. Future reports will provide detailed information regarding the various forms of degradation measured in soft and hard piezoelectric materials.

References

Aoki K and K Fukuda, Jpn J Appl Phys, 36, 1997, L1195-97.
Audigier A et. Al. Ferroelectrics, 1994, Vol. 154, pp219-224
Berlincourt D A, J Appl Phys, 30, 11, pp1804-1810 (1959).
CMMT A(98) Cain MG, Stewart S, Gee M
CMMT A(99) Cain MG, Stewart S, Gee M
Cao H and A G Evans, J Am Ceram Soc, 76, 1993, 890-96.
Chen T-C et al, J Materials Research, V12, N10, 1997, pp2628-2637.
Damjanovic D et al, Sensors and Actuators A 53, 353-360 (1996)
Damjanovic D et al. J Phys: Conden Matter 9, 4943-4953 (1997)
Damjanovic D et al., J Phys D: Appl Phys 29, 2057-2060 (1996)
Damjanovic D Phys Rev B Condensed Matter Vol 55, N2, R649-652 (1997)
Duiker J M etal., J Appl Phys 68, 5783 (1990)
Freeman A and S P Joshi, SPIE, 2715, 1996, 602-613.
Hall D, J. Phys: Condens. Matter, 10, 461-476 (1998)
Hennig E and P Pertsch, Actuator 96, p249-252, 5th International Conference on New Actuators, 26-28 June, Bremen, Germany.
Hill M D, G S White, and C-S Hwang, J Am Ceram Soc, 79, 1996, 1915-20.
Jiang Q Y, LE Cross, J Mater Sci., 28, 4536, (1993).
Jonker G H, J Am Ceram Soc, 55, 1972, 57-58.
Krueger H H A, J Acoust. Soc. Am., 42, 1967, 636-45.
Krueger HHA, J Acoust Soc Am, Vol.42, No. 3, 1967 pp636-645.
Kudzin A Y et al. Sov. Phys. Solid State 16, 1589 (1975)
Li S et al. J. Appl. Phys., 69, 7219-24
Meeks S W, J App Phys 46, 10, Oct 1975. Pp4334-4338
Michelis Dr Paul, IMMG, Penteli, Athens, Greece. Personal Communication.
Morgan Matroc Ltd., Piezoelectric Ceramics, Transducer Products Division, Thornhill, Southampton.
Pertsch P, F Borisch, G Borchhardt, B Hofer, H Rohr, and E Wehrsdorfer, Actuator 96, p217-220, 5th International Conference on New Actuators, 26-28 June, Bremen, Germany.
Robels U et al, Ferroelectrics, 133, 163-8
Shaufele A B and K H Hardtl, J Am Ceram Soc, 79, 1996, 2637-40.
Sherrit S et al, SPIE, vol.3040., pp99-109. 1997
Warren W L et al., J Am Ceram Soc., 77 (10), 2753 (1994)
Warren W.L, D Dimos, and R. M Waser, MRS Bulletin, 21, July 1996, 40-45
Waser R, T Baiatu, and K H Hardtl, J Am Ceram Soc, 73, (1990), 1645-53.
Wu K et al., J. Am. Ceram. Soc., 75, 3385-9

Appendix 1: Experimental Plan and questionnaire returns.

An extensive scientific questionnaire was formulated by NPL and distributed to all members of CAM7 Industrial Advisory Group. The feedback generated was used in the formulation of the testing envelope that was subsequently used for the work reported in this document:

Materials

Morgan Matroc Unilator Hard and Soft, 4D 6 and 5H 6
Morgan Matroc TPD Hard and Soft, 4D 5 and 5A 5
Advanced Ceramic hot pressed, 4040 (4D like) 4 and 4050 (5 type) 5

Static Loading Measurements under static stresses

High and low field Capacitance and loss measurements at 1kHz with static stresses of 1.3, 13, 64, 127, 254MPa 8
P- E loop measurements at frequencies of 0.1, 1, 10, 100, 1000Hz with static stresses 1.3, 13, 64, 127, 254MPa 4
Displacement-Field measurements at frequencies of 0.1, 1, 10, 100, 1000Hz with static stresses of 1.3, 13, 64, 127, 254MPa 7

Mechanical Cyclic Loading

Application of AC mechanical stress and measure the charge output.
d33 measurements at 0.1, 1, 10, 100, 1000Hz and cyclic stresses of 0.64, 1.3, 6.4, 12.7, 25.5MPa 8
with simultaneous displacement measurement 8

Mechanical Fatigue

Hard - 5, 15, 30 , 60MPa cycles up to 108 cycles at frequencies 1, 10 and 100Hz 7
Soft - 1, 5, 10, 20MPa cycles up to 108 cycles at frequencies 1, 10 and 100Hz 4

- Measure Charge-Stress loops 2
- Measure Displacement Stress loops 7
- Interrupt loading + measure low field capacitance 1
- Remove some samples for d33, keff, P-E, D-E, etc 5
- look at open and short circuit conditions 2

Electrical Fatigue

Application of AC field for a number of cycles and measure performance (additionally with static mechanical clamping stress).
Hard 0.5, 1.0, 1.5 kV/mm at 1,10, 100 and 1000Hz with clamping stresses of 0, 40 and 80MPa up to 109 cycles 8
Soft 0.5, 1.0, 1.5 kV/mm at 1,10, 100 and 1000Hz with clamping stresses of 0, 10 and 20MPa up to 109 cycles 8

- Measure P-E loops 5
- Measure high field capacitance and loss 5
- Measure displacement field loops 8

Remove some samples for d33, keff, P-E, D-E, high field capacitance etc 7